RESEARCH ARTICLE

Figures and figure supplements

Myoglobin-derived iron causes wound enlargement and impaired regeneration in pressure injuries of muscle

Nurul Jannah Mohamed Nasir *et al*.

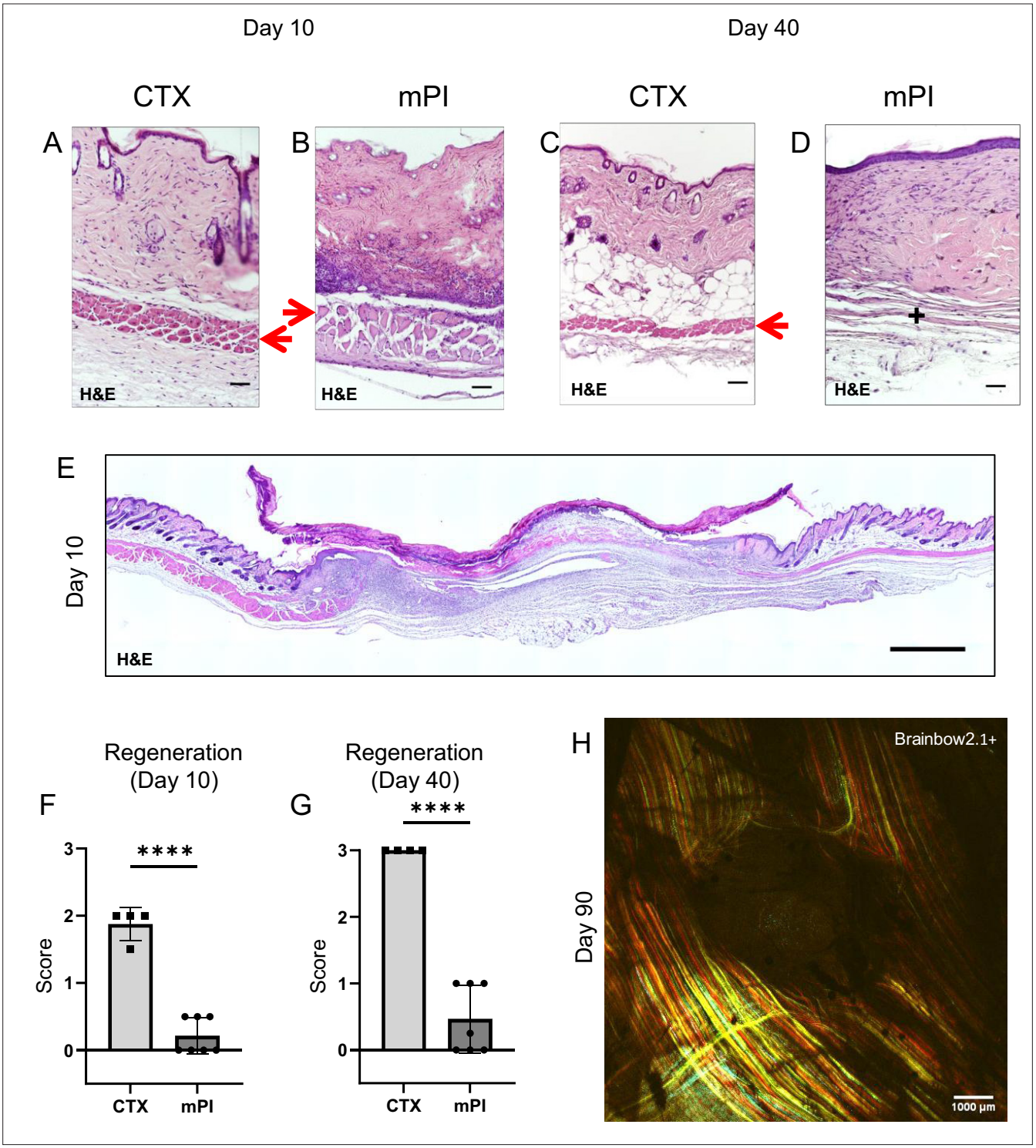

Figure 1. Poor regeneration of muscle pressure injury (mPI), a model of chronic wound, compared with cardiotoxin (CTX), a model of acute injury. H&E-stained sections of saline-treated wound tissues (**A, B**) at day 10 post-injury and (**C, D**) day 40 post-injury. Red arrows point to the panniculus carnosus layer. '+' indicates where the panniculus layer should be. Scale bars: 50 µm. Uninjured control tissue, stained with H&E, is shown in ***Supplementary file 1C***. (**E**) Full cross-section of H&E-stained mPI, including uninjured edges, at day 10 post-injury. Note the eschar attached to the wound surface. Scale bar: 500 µm. (**F, G**) Comparison of the regeneration scores for the panniculus layer between mPI and CTX injuries at days 10 and 40. (**H**) A multi-channel confocal image of the panniculus layer shows a round hole remains in the muscle, 90 d after mPI. Scale bar: 1000 µm. All injuries are saline-treated to permit comparison against later mPI treatments. All quantitative data are reported as means ± SD. n = 4–7. ****<0.0001 Statistical significance in (**F**) and (**G**) was computed by unpaired Student's *t* test.

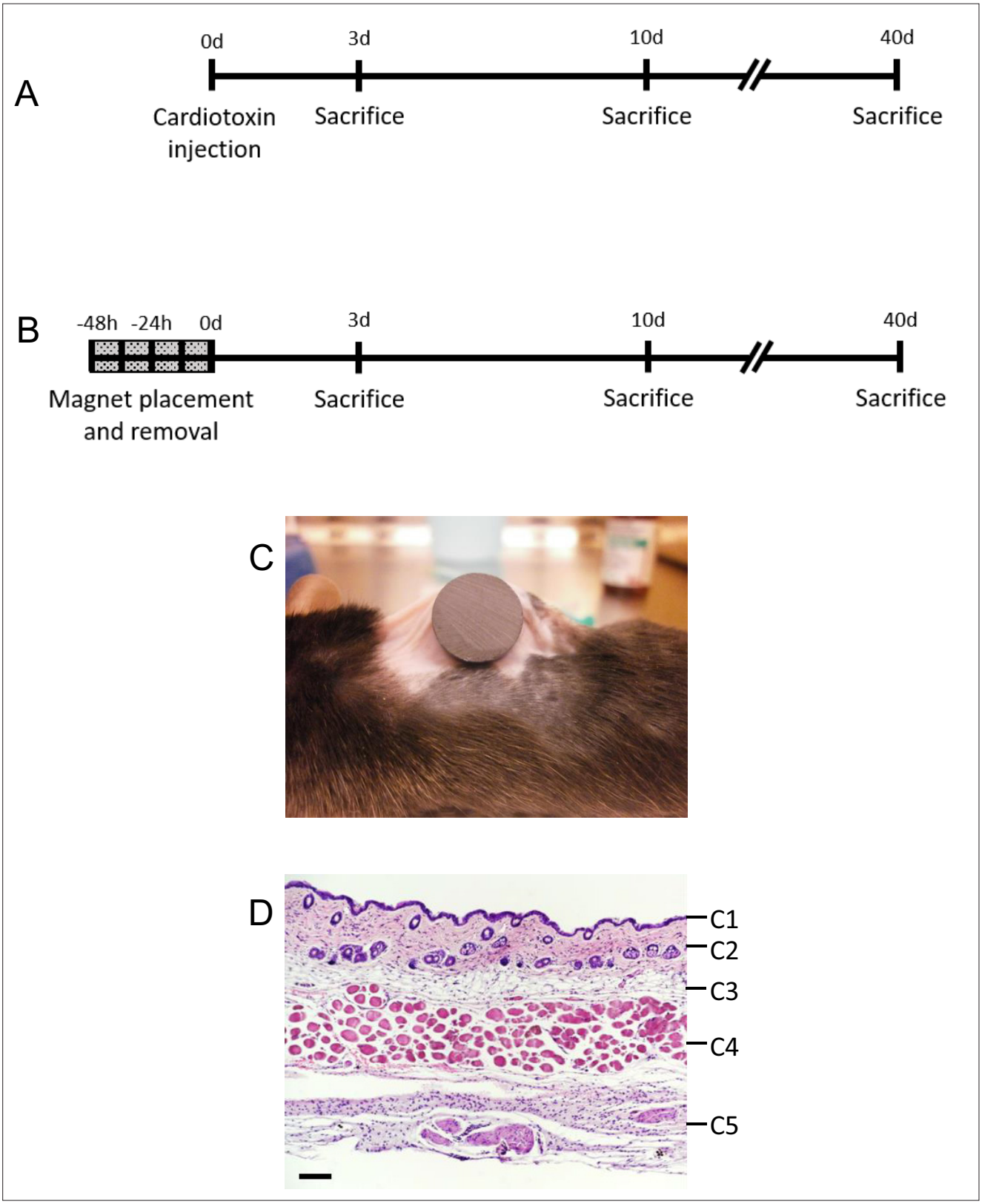

Figure 1—figure supplement 1. Mouse model of injury. (**A**) Experimental schedule of cardiotoxin acute injury and tissue collection. (**B**) Experimental schedule of muscle pressure injury (mPI) induction and tissue collection. (**C**) Image of mPI induction in C57BL6 mouse with a 12 mm magnet on the dorsal skinfold. (**D**) An H&E-stained cross-section of healthy murine dorsal skinfold, showing the epidermis (C1), dermis (C2), dermal white adipose tissue (dWAT) (C3), panniculus carnosus muscle (PC) (C4), and loose areolar tissue (C5). Scale bar is 50 μm.

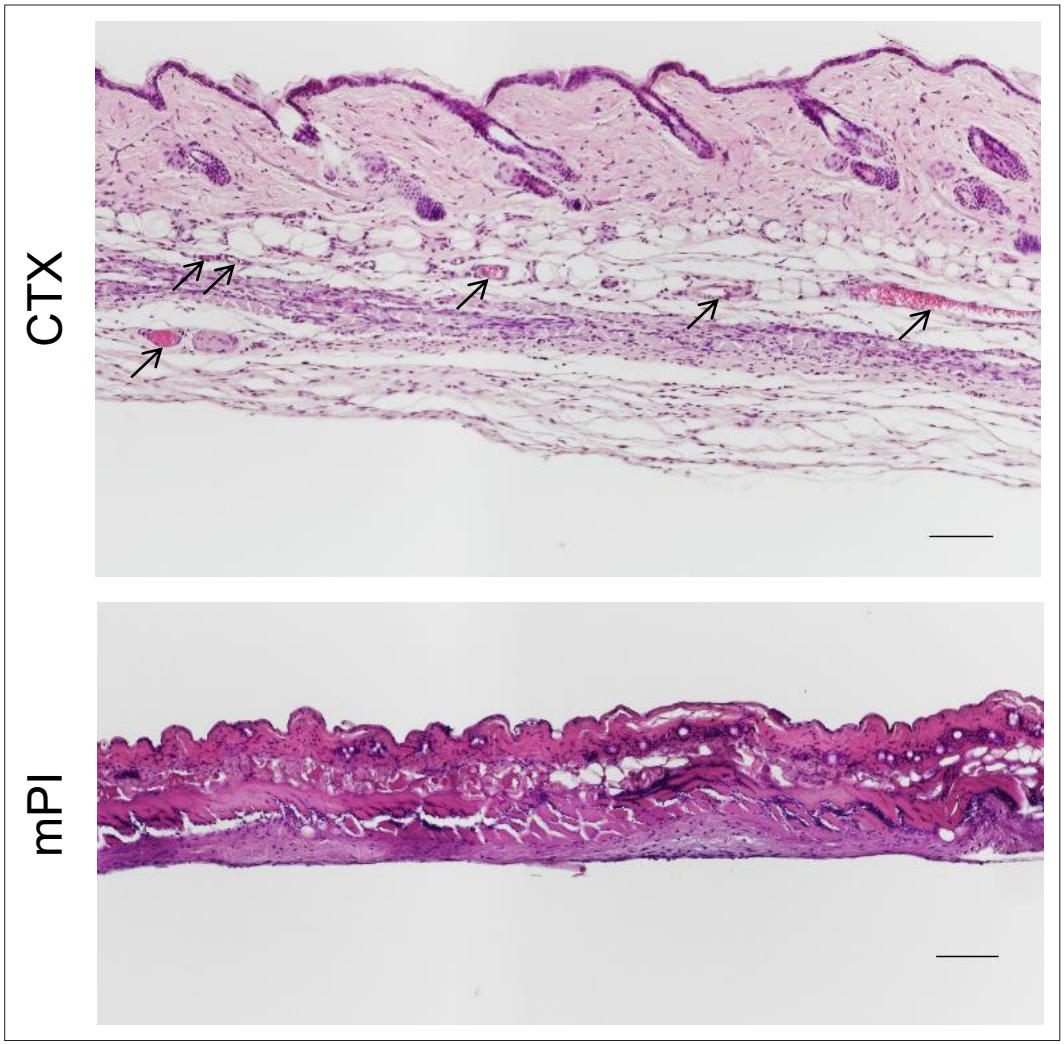

Figure 1—figure supplement 2. Intact blood vessels are absent or infrequent in the dead tissue of muscle pressure injuries (mPI). H&E sections of cardiotoxin (CTX)-injured tissue (top) versus mPI (bottom) at day 3. Black arrows point to intact capillaries in the skinfold. Scale bars: 100 μm.

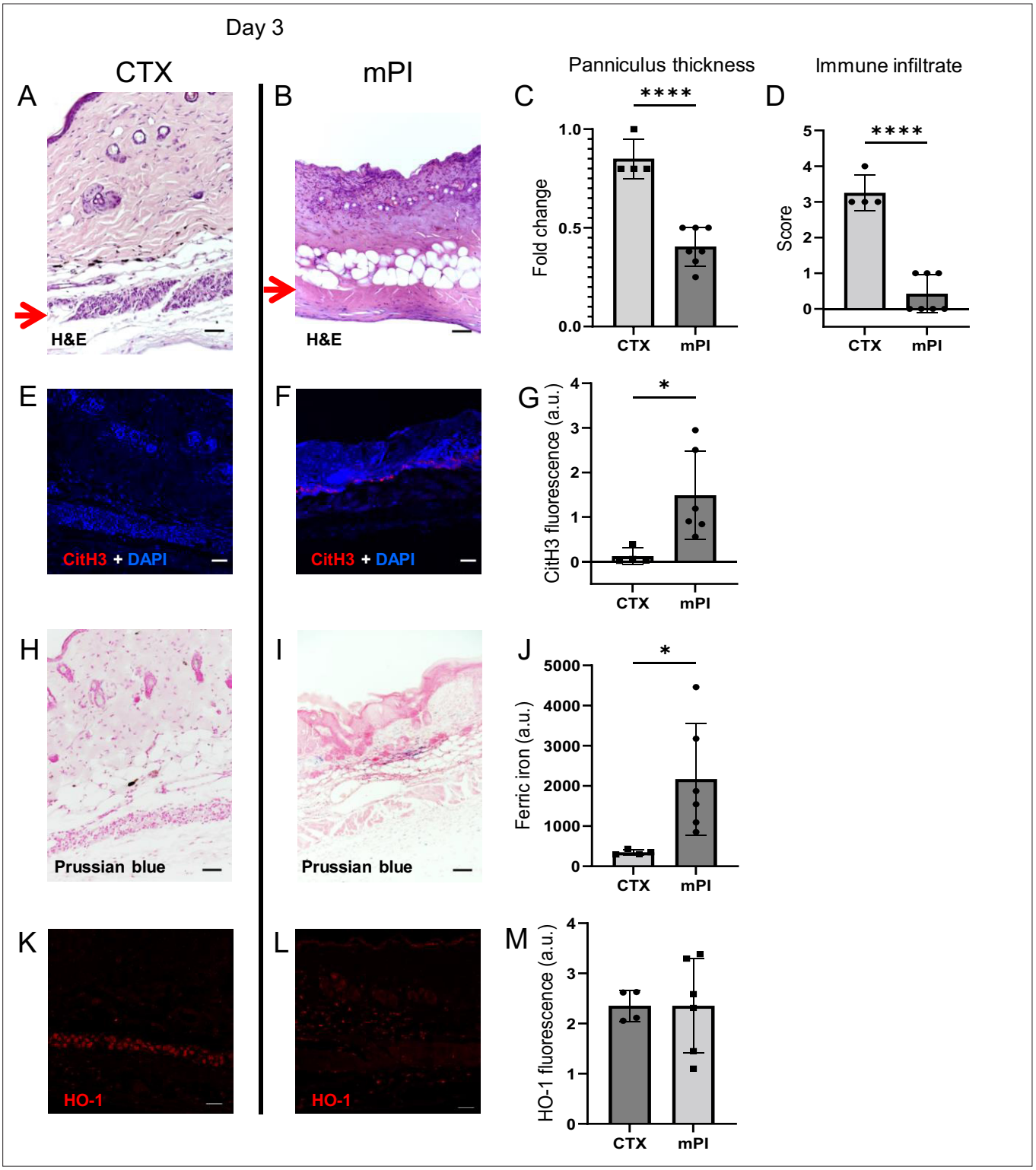

Figure 2. Early-stage pathologies in the injury-response of muscle pressure injury (mPI) (3 d after injury). (**A, B**) H&E-stained sections of saline-treated wound tissues, comparing magnet-induced mPI versus cardiotoxin (CTX) injury. Red arrows point to the panniculus carnosus (PC) layer. (**C**) Thickness of PC layer. (**D**) Histopathology scoring of immune infiltrate into the injured PC layer. (**E, F**) Immunostaining for citrullinated histone-3 (CitH3, a marker for extracellular traps, in red) in mPI versus CTX. DNA/nuclei were co-stained blue with DAPI. (**G**) Quantification of CitH3 staining. (**H, I**) Perls' Prussian blue iron staining (dark blue-gray), with nuclear fast red co-stain. (**J**) Quantification of Perls' staining. (**K, L**) Immunostaining for heme oxygenase-1 (HO-1, a marker of heme and iron) in mPI versus CTX. Note that the HO-1-positive signal in CTX injury is localized to the panniculus carnosus and is widespread across all layers in mPI. (**M**) Quantification of HO-1 staining. Scale bars: 50 μm. All quantitative data are reported as means ± SD. n = 4–7 mice. *<0.05, ****<0.0001. Statistical significance in (**C, D**), (**G**), (**J**), and (**M**) was computed by unpaired Student's *t* test.

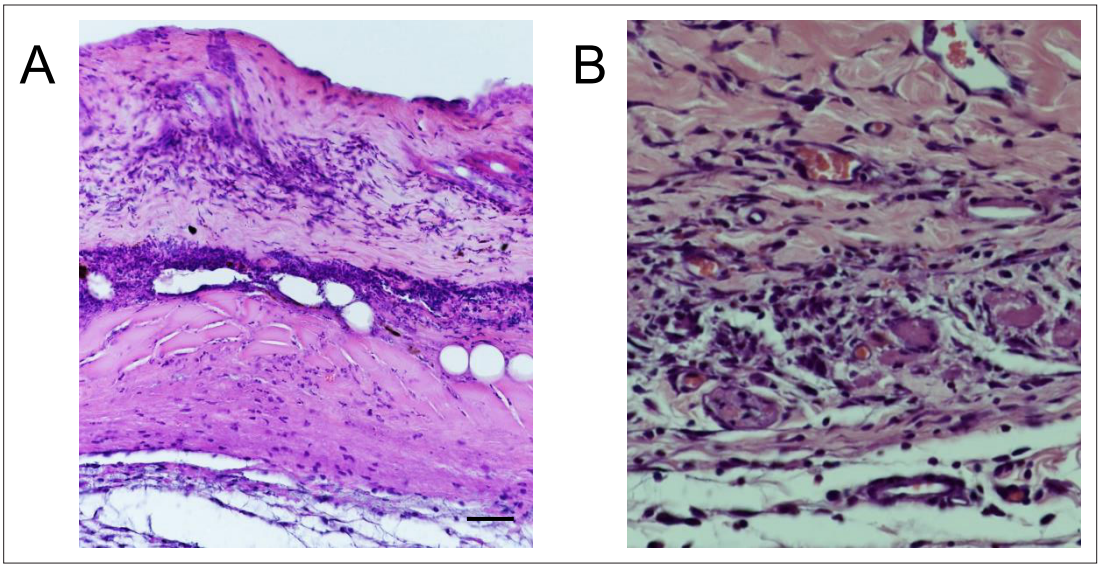

Figure 2—figure supplement 1. Wound margins show intact immune cells but the compressed region of muscle pressure injury (mPI) lack viable immune infiltrate. (**A**) A cross-section of mPI at day 3 post-injury, stained with H&E showing indicators of cell death (karyolysis, karyorrhexis, and acidification), and a lack of intact immune cells in the compressed region. (**B**) Another cross-section taken from the wound edge (boundary between injured and uninjured tissue) showing intact immune cell infiltrate. Scale bar is 25 μm.

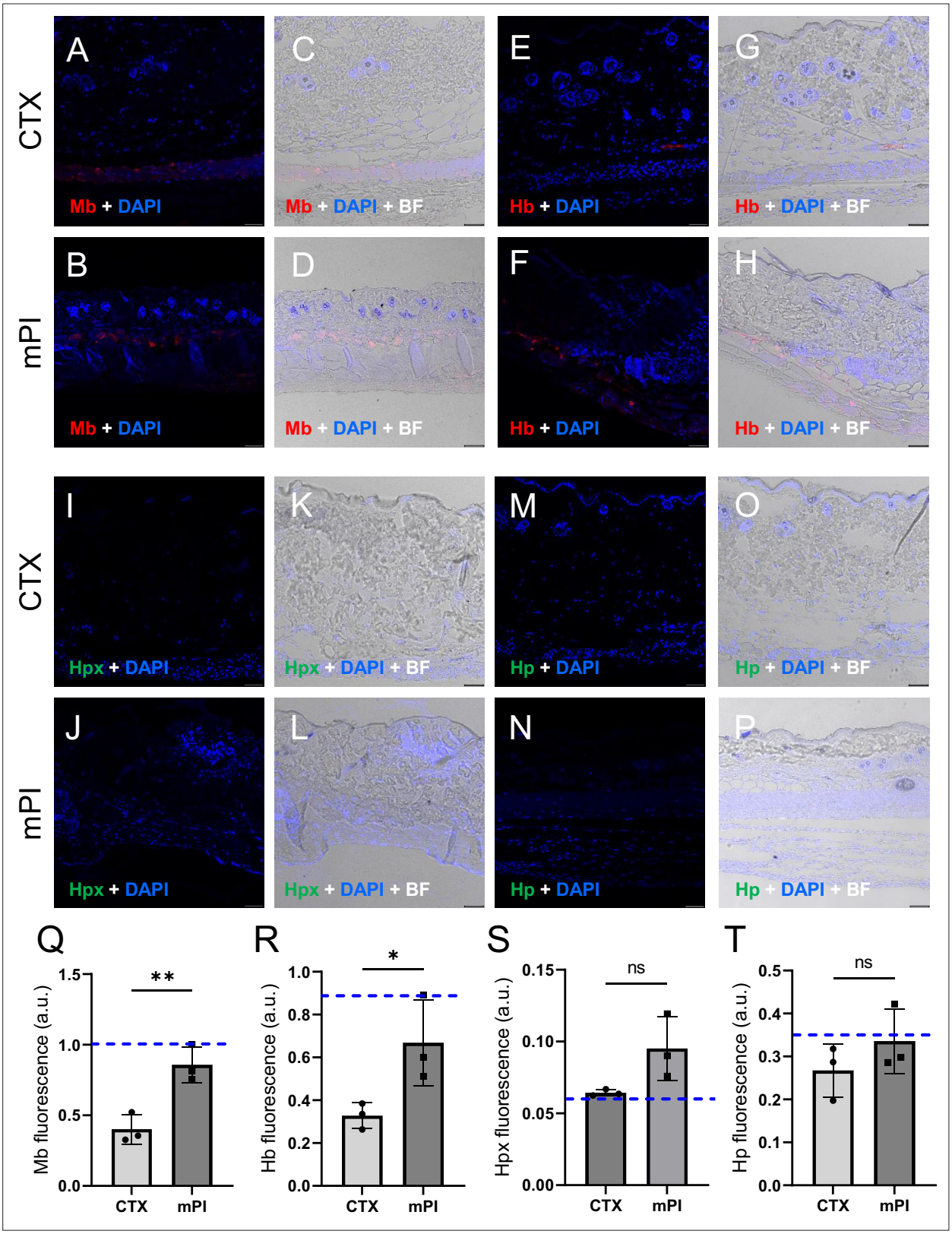

Figure 2—figure supplement 2. Levels of globin-proteins and iron detoxification factors 3 d after cardiotoxin (CTX) injury and muscle pressure injury (mPI). Immunostaining of (**A–D**) myoglobin (Mb), (**E–H**) hemoglobin (Hb), (**I–L**) hemopexin (Hpx), and (**M–P**) haptoglobin (Hp) in CTX versus mPI tissues. Note that day 3 might be too late to see the peak of iron detoxification for the CTX injury, and the damaged vasculature of mPI might decrease the influx of iron detoxification factors into high-iron mPI wounds. (**C**), (**D**), (**G**), (**H**), (**K**). (**L**), (**O**), and (**P**) are images merged with brightfield

Figure 2—figure supplement 2 continued on next page

Figure 2—figure supplement 2 continued

of (**A**), (**B**), (**E**), (**F**), (**I**), (**J**), (**M**), and (**N**), respectively. Scale bars are 50 μm. (**Q–T**) Quantification of Mb, Hb, Hpx, and Hp staining. All injuries are saline-treated. Blue dotted line indicates average fluorescence in uninjured skinfold. Mean ± SD. n = 3 mice. *<0.05, **<0.01. Statistical significance was computed by unpaired Student's *t* test.

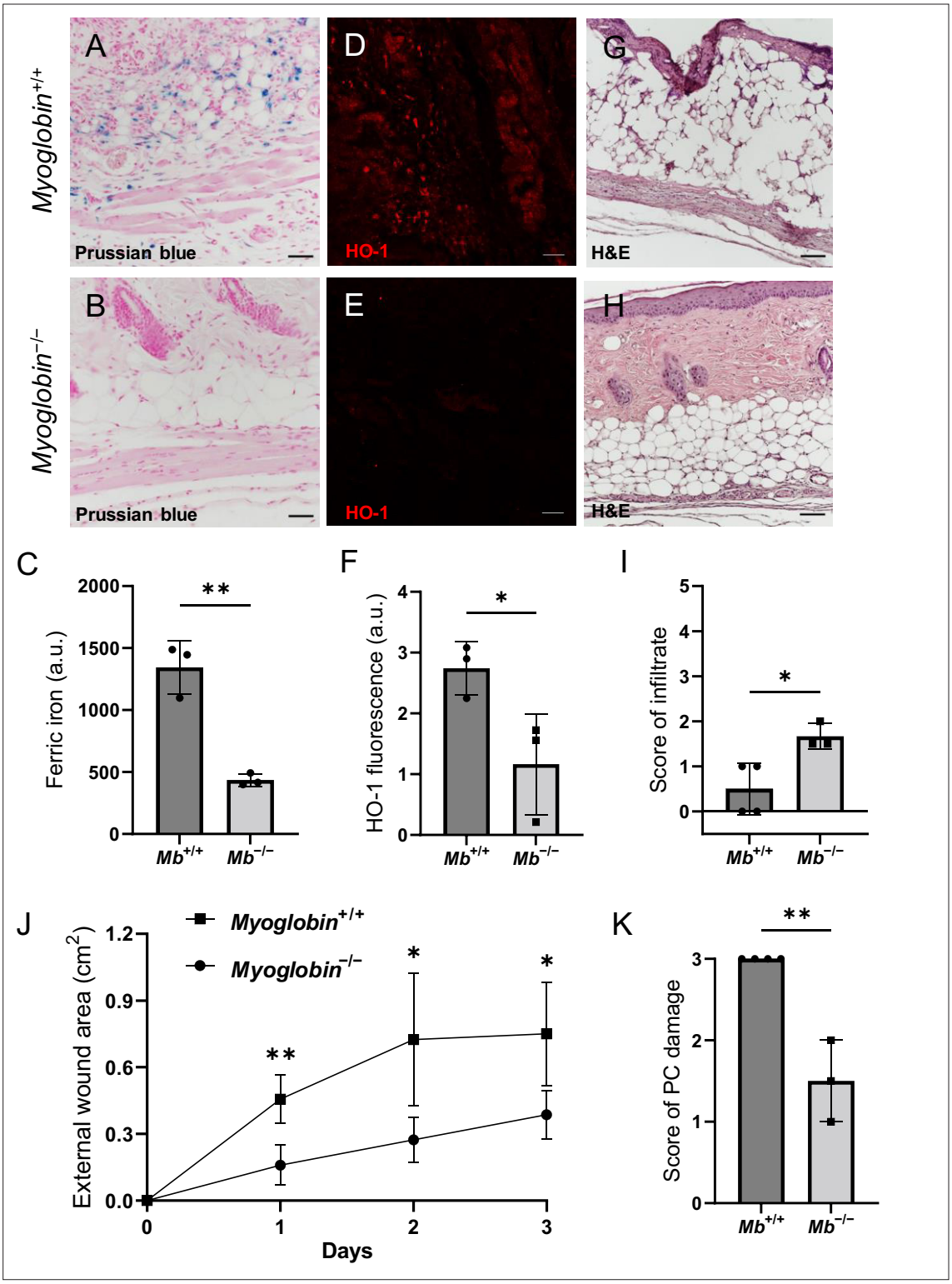

Figure 3. Myoglobin knockout decreased iron deposits and tissue death after muscle pressure injury (mPI). (**A, B**) Perls' Prussian blue iron staining. (**A**) Note that iron deposits in the extracellular space and in immune cells of $Mb^{+/+}$ wound tissue, and note that (**B**) $Mb^{-/-}$ tissues have no iron deposits in extracellular regions. (**C**) Quantification of Perls' staining. (**D, E**) Immunostaining for HO-1 in $Mb^{+/+}$ versus $Mb^{-/-}$ tissues at day 3 after mPI. Note that HO-1 is elevated in all layers of $Mb^{-/-}$ except epidermis. (**F**) Quantification of HO-1 immunostaining. (**G, H**) H&E-stained sections of $Mb^{+/+}$ versus $Mb^{-/-}$ mPI. Paraffin-embedded wound sections derived from elderly Mb-wildtype mice had poor cohesiveness (compared to elderly Mb-knockout or young) and exhibited greater cracking during identical sample handling. (**I**) Amount of immune infiltrate, quantified by histopathology scoring on a scale of 0–5,

Figure 3 continued on next page

Figure 3 continued

performed on day 3 sections. (**J**) External wound area in $Mb^{+/+}$ and $Mb^{-/-}$ mice in the initial days following mPI from 12 mm magnets. Statistical analysis compared four wounds from two age- and sex-matched animals using a Student's *t* test for each day. Consistent with these results, ***Supplementary file 1C*** shows additional animals treated with different-sized magnets. (**K**) Tissue death in the PC muscle layer by histopathology scoring (3 indicates pervasive death). All quantitative data are reported as means ± SD. n = 3 mice. *<0.05, **<0.01. Statistical significance in (**C**), (**F**), and (**I–K**) was computed by unpaired Student's *t* test.

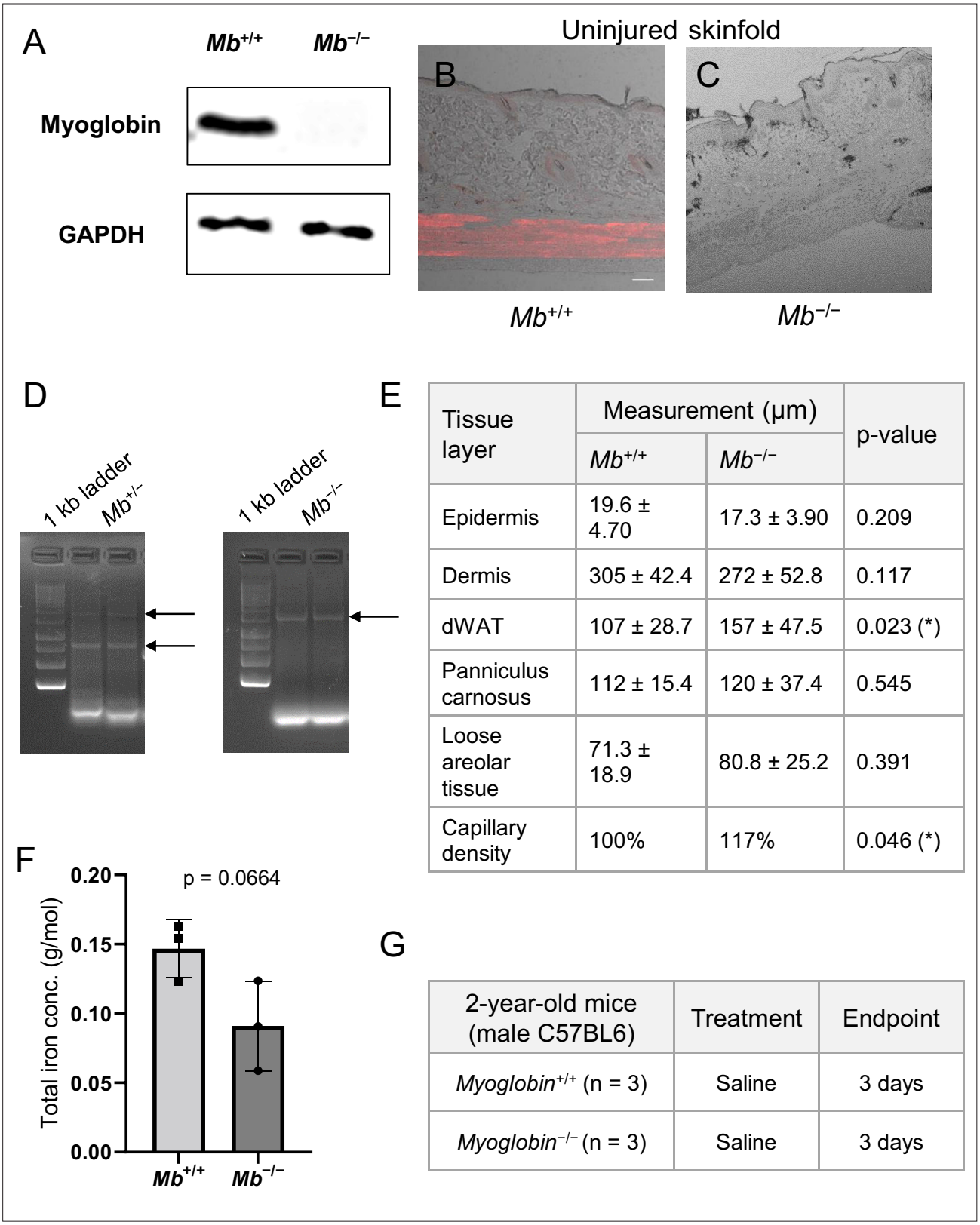

Tissue layer	Measurement (µm)		p-value
	Mb$^{+/+}$	*Mb*$^{-/-}$	
Epidermis	19.6 ± 4.70	17.3 ± 3.90	0.209
Dermis	305 ± 42.4	272 ± 52.8	0.117
dWAT	107 ± 28.7	157 ± 47.5	0.023 (*)
Panniculus carnosus	112 ± 15.4	120 ± 37.4	0.545
Loose areolar tissue	71.3 ± 18.9	80.8 ± 25.2	0.391
Capillary density	100%	117%	0.046 (*)

2-year-old mice (male C57BL6)	Treatment	Endpoint
Myoglobin$^{+/+}$ (n = 3)	Saline	3 days
Myoglobin$^{-/-}$ (n = 3)	Saline	3 days

Figure 3—figure supplement 1. Validation of myoglobin-knockout mice. (**A**) Western blotting in panniculus carnosus homogenate to validate the myoglobin levels of *Mb*$^{+/+}$ and *Mb*$^{-/-}$ mice (one blot for every mouse). (**B, C**) Myoglobin immunostaining (red) in the uninjured skinfold to validate the myoglobin levels of *Mb*$^{+/+}$ and *Mb*$^{-/-}$ mice (at least four samples per mouse). Scale bars are 50 µm. (**D**) Gel electrophoresis bands from PCR amplification of *Mb*$^{-/-}$ (1700 bp; top arrows) and *Mb*$^{+/+}$ (648 bp; bottom arrow) from mouse genomic DNA. (**E**) Morphological comparison of the dorsal skinfolds

Figure 3—figure supplement 1 continued on next page

Figure 3—figure supplement 1 continued

(measured from H&E sections) in $Mb^{+/+}$ and $Mb^{-/-}$ mice. (**F**) Quantification of total iron in *tibialis anterior* muscles in $Mb^{+/+}$ and $Mb^{-/-}$ mice. (**G**) Table of treatment arms. Mean ± SD. n = 3 mice. *<0.05. Statistical significance was computed by unpaired Student's *t* test.

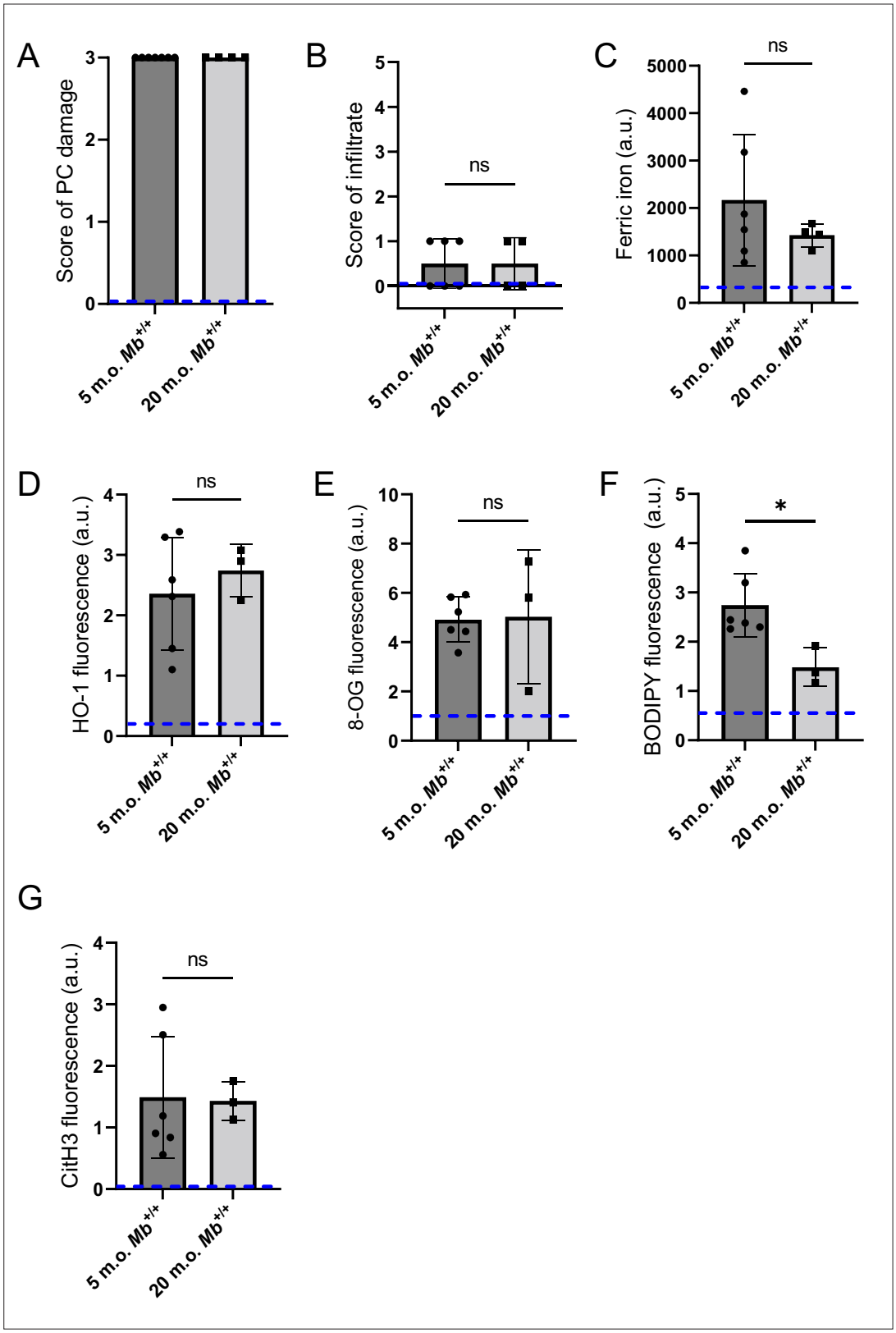

Figure 3—figure supplement 2. Comparison of muscle pressure injury (mPI) in young and elderly mice. Readouts of the wound environment: (**A**) Tissue death in the panniculus carnosus, (**B**) immune cell infiltration, (**C–F**) oxidative stress, and (**G**) the CitH3 marker. All were measured at day 3 after mPI in 5-month-old versus 20-month-old myoglobin-wildtype mice. Uninjured control tissue (young) is also shown as a zero baseline. Mean ± SD. n = 4–6 mice. ns, not significant, *<0.05. Statistical significance was computed by unpaired Student's *t* test.

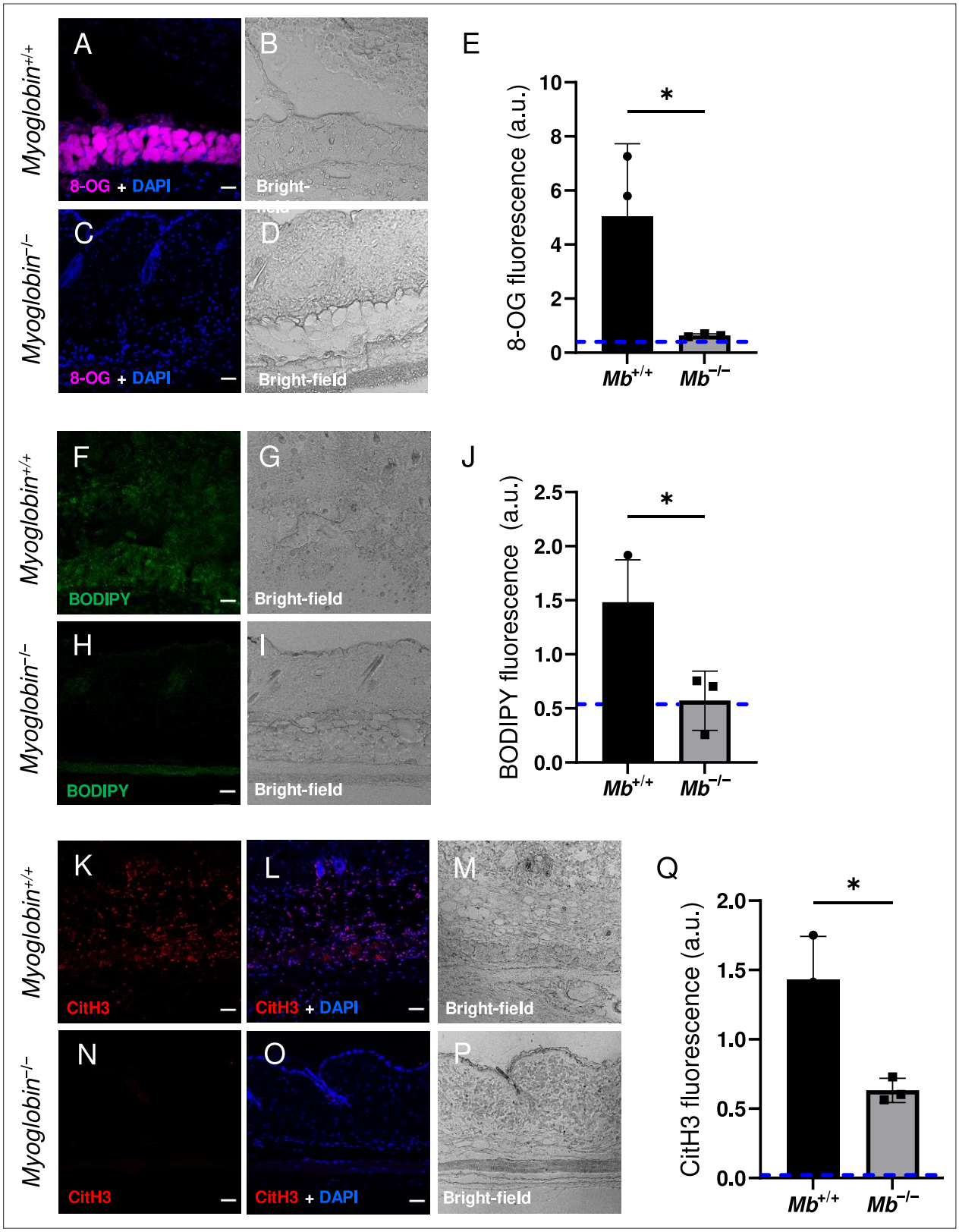

Figure 4. Myoglobin knockout caused a more hospitable wound environment in muscle pressure injury (mPI). (**A–D**) Immunostaining of 8- oxaguanine (8-OG; in magenta) in $Mb^{+/+}$ versus $Mb^{-/-}$ mPI. Nuclei were co-stained blue with DAPI. (**B**) and (**D**) are brightfield images of (**A**) and (**C**), respectively. (**E**) Quantification of 8-OG staining. (**F–I**) BODIPY staining (for lipid peroxidation) in $Mb^{+/+}$ versus $Mb^{-/-}$. (**G**) and (**I**) are brightfield images of (**F**) and (**H**), respectively. (**J**) Quantification of BODIPY staining. (**K–P**) Immunostaining for CitH3 (in red) in $Mb^{+/+}$ versus $Mb^{-/-}$. (**L, O**) DNA/nuclei were co-stained

Figure 4 continued on next page

Figure 4 continued

blue with DAPI. (**M**) and (**P**) are brightfield images of (**K**) and (**N**), respectively. (**Q**) Quantification of CitH3 staining. Scale bars: 50 μm. Blue dashed lines refer to mean fluorescence intensities for uninjured dorsal skinfolds. All quantitative data are reported as means ± SD. n = 3 mice. *<0.05. Statistical significance in (**E**), (**J**), and (**Q**) was computed by unpaired Student's *t* test.

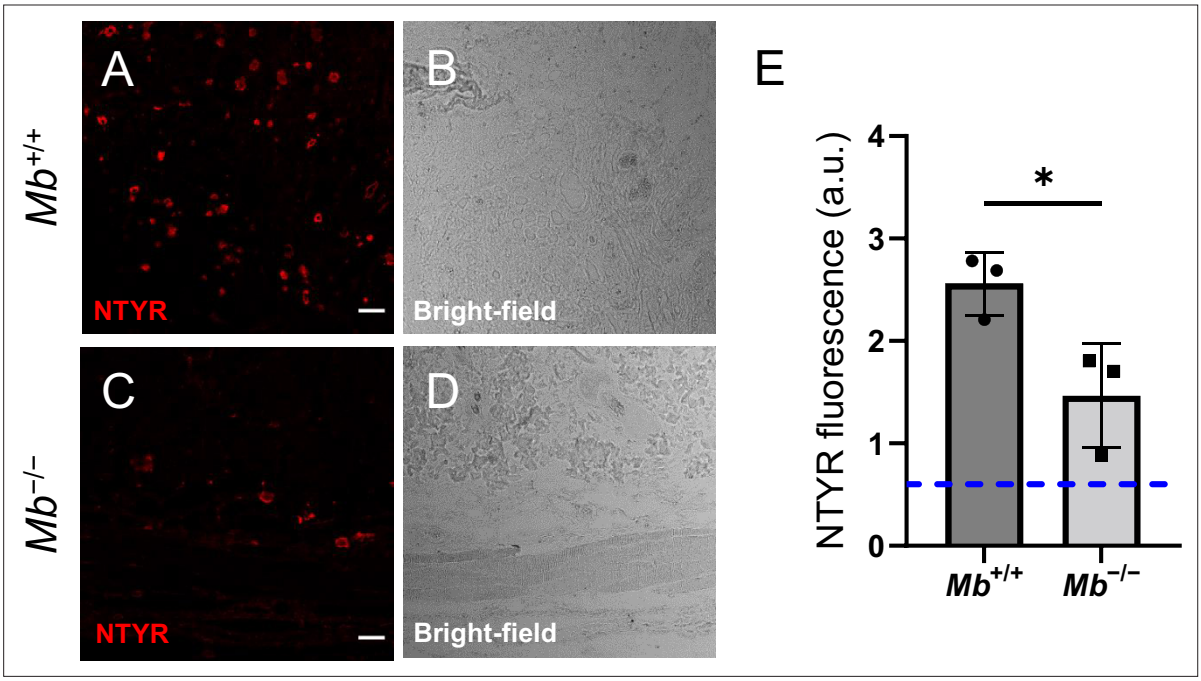

Figure 4—figure supplement 1. Nitroxidative stress in $Mb^{+/+}$ versus $Mb^{-/-}$ tissues 3 d after muscle pressure injury (mPI). (**A–D**) Immunostaining of nitrotyrosine (NTYR), a marker of nitroxidative stress, in $Mb^{+/+}$ versus $Mb^{-/-}$ pressure-injured tissues. (**B**) and (**D**) are brightfield images of (**A**) and (**C**), respectively. Scale bars are 50 μm. (**E**) Quantification of NTYR staining. Blue dotted line indicates average NTYR fluorescence in uninjured skinfold. Mean ± SD. n = 3 mice. *<0.05. Statistical significance was computed by unpaired Student's *t* test.

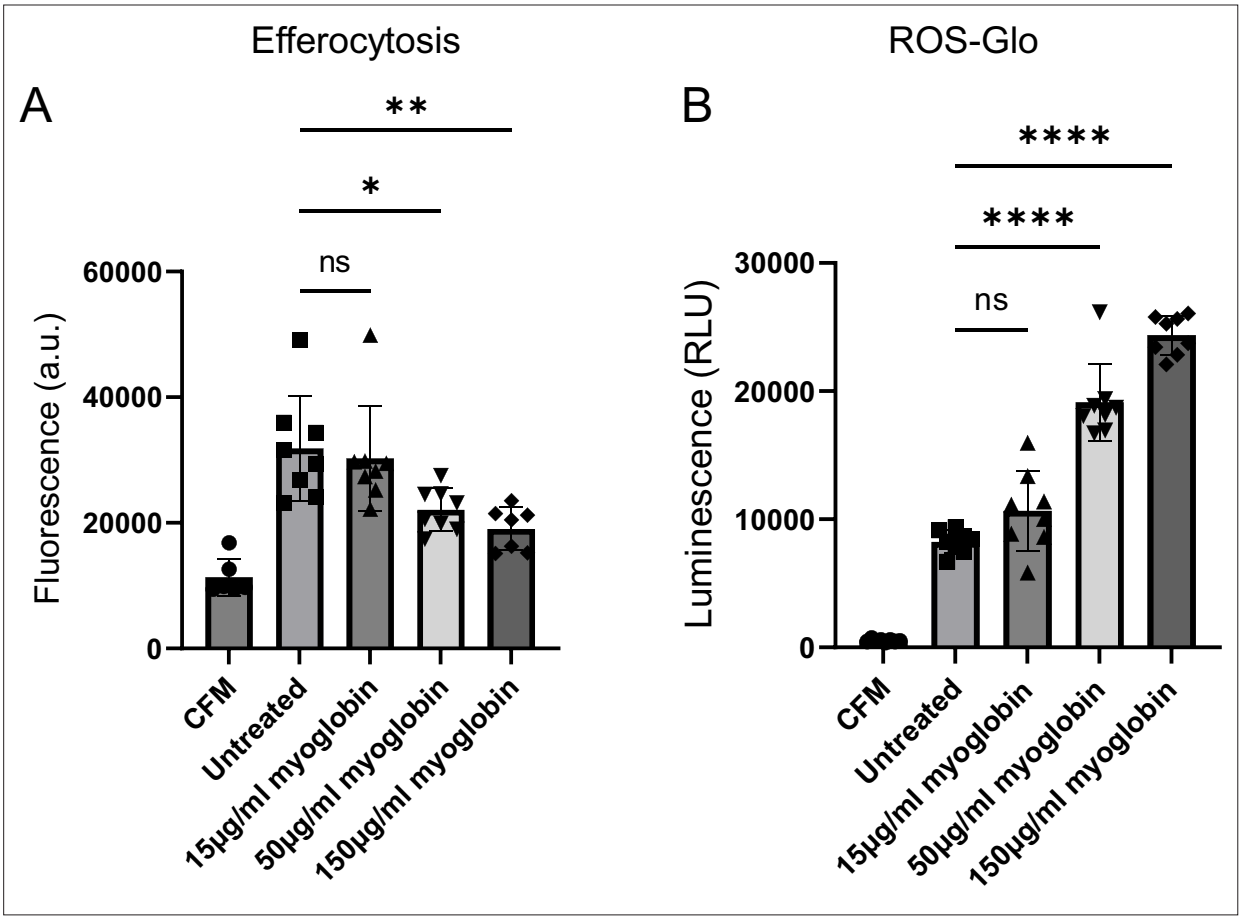

Figure 4—figure supplement 2. Extracellular myoglobin increases reactive oxygen species (ROS) in and decreases the function of macrophages in vitro. RAW 264.7 monocyte cells were incubated with pro-inflammatory stimuli (10 ng/ml IFNγ + 100 ng/ml LPS) to induce M1-like macrophage differentiation, prior to treatment with varying concentrations of myoglobin for 24 hr. (**A**) An efferocytosis measure (of engulfed CFSE-labeled fluorescent myoblast apoptotic bodies), and (**B**) an oxidative stress measure (ROS-Glo H_2O_2 assay). Positive control used 100 µM menadione in DMSO, with luminescence (not plotted) of 175000. CFM = cell-free media. n = 7–8 replicates. Mean ± SD. 'ns,' not significant, *<0.05, **<0.01, ****<0.0001. Statistical significance was computed by one-way analysis of variance (ANOVA) with Tukey's post hoc test.

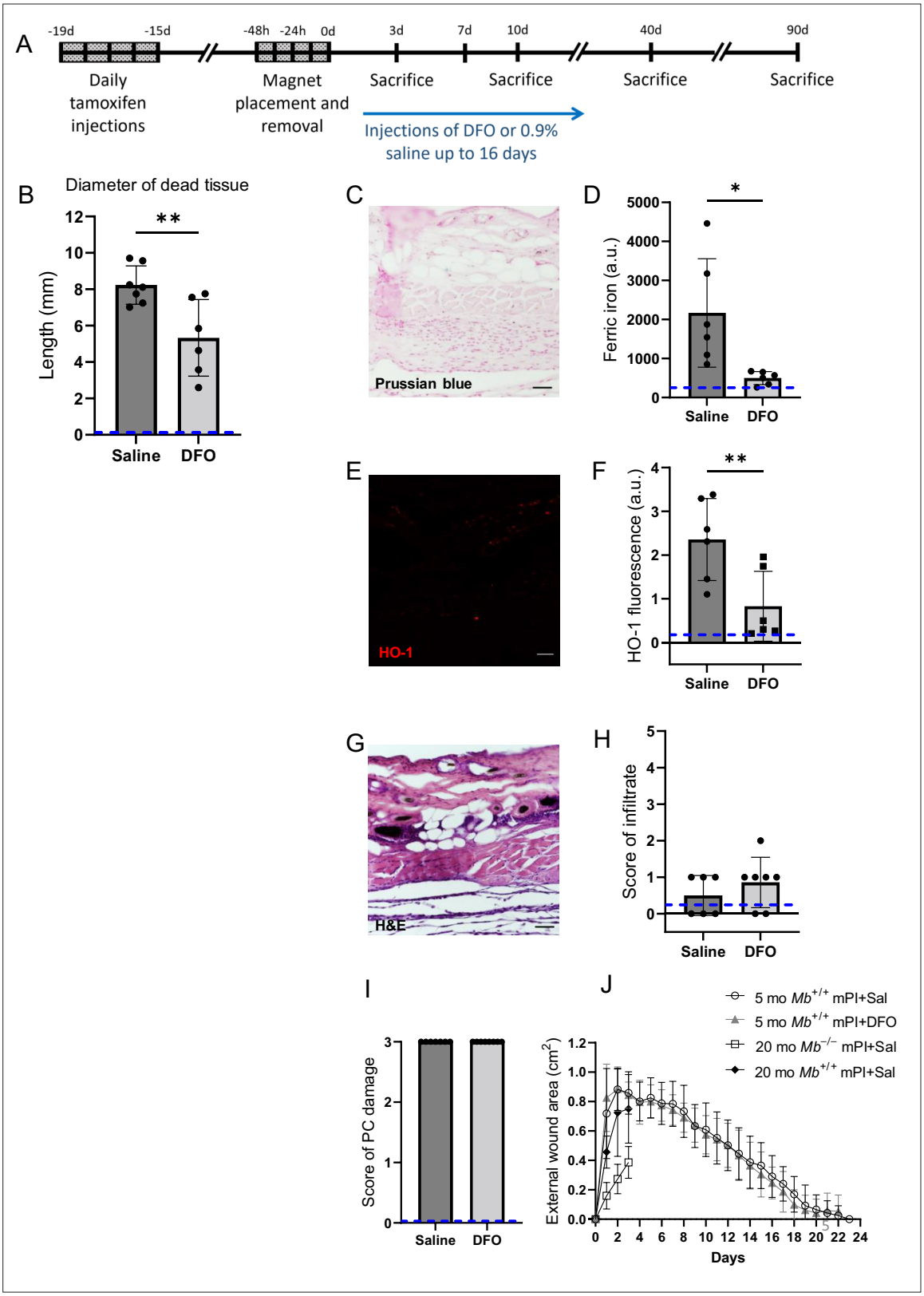

Figure 5. Deferoxamine (DFO) iron chelation therapy decreased iron deposits at day 3 after muscle pressure injury (mPI). (**A**) Experimental schedule shows confetti tamoxifen induction of fluorescence, mPI induction, treatment with DFO or saline, and tissue harvest. (**B**) Diameter of the dead region of the panniculus carnosus (PC) muscle in tissue sections from DFO- versus saline-treated mPI, 3 d post-injury. (**C**) Perls ' Prussian blue iron staining of DFO-treated wounds at the wound center. (**D**) Quantification of Perls ' staining, showing comparison against saline-treated mPI from ***Figure 2I***.

Figure 5 continued on next page

Figure 5 continued

(**E**) Immunostaining of HO-1 in DFO-treated mPI. (**F**) Quantification of HO-1 staining, showing comparison against saline-treated mPI from ***Figure 2L***. (**G**) H&E-stained sections of DFO-treated mPI at the wound center. (**H**) Histopathology scoring of immune infiltrate at all layers of the wound center at day 3, comparing DFO-treated versus saline-treated mPI, which appear in ***Figure 2B and (D***). (**I**) Confirmation that injuries were properly created, according to death of PC tissue at the center of the wound (histopathology scoring where 3 indicates pervasive tissue death). (**J**) Skin wound area following mPI in 5-month-old $Mb^{+/+}$ saline and DFO-treated mice, and in 20-month-old $Mb^{+/+}$ and $Mb^{-/-}$ saline-treated mice. Scale bars: 50 μm. Blue dashed lines refer to histology scores and mean fluorescence intensities for uninjured dorsal skinfolds. All quantitative data are reported as means ± SD. n = 6–7 mice. *<0.05, **<0.01. Statistical significance in (**B**), (**D**), (**F**), and (**H–J**) was computed by paired Student's *t* test.

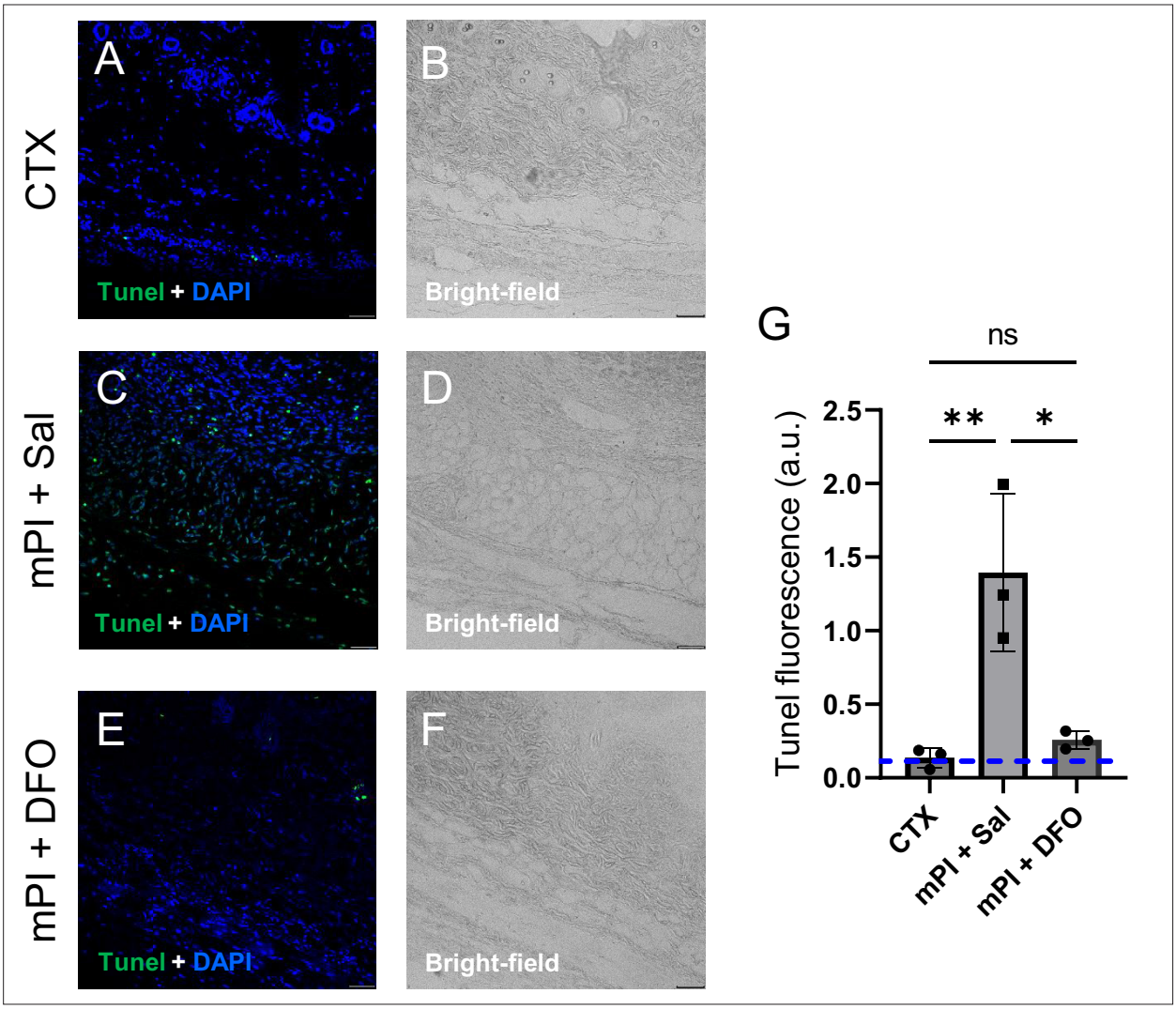

Figure 5—figure supplement 1. Saline-treated muscle pressure injury (mPI) show increased TUNEL staining compared to deferoxamine (DFO)-treated mPI and cardiotoxin (CTX) injury. (**A–F**) TUNEL staining in CTX, saline-treated mPI, and DFO-treated mPI. (**B**), (**D**), and (**F**) are brightfield images of (**A**), (**C**), and (**E**), respectively. Note that the increased TUNEL staining might have arisen from increased production (e.g., secondary progression of the wound) or from decreased uptake (e.g., impaired efferocytosis). Scale bars are 50 μm. (**G**) Quantification of TUNEL staining. Mean ± SD. n = 3 mice. *<0.05, **<0.01. Statistical significance was computed by one-way analysis of variance (ANOVA) with Tukey's post hoc test.

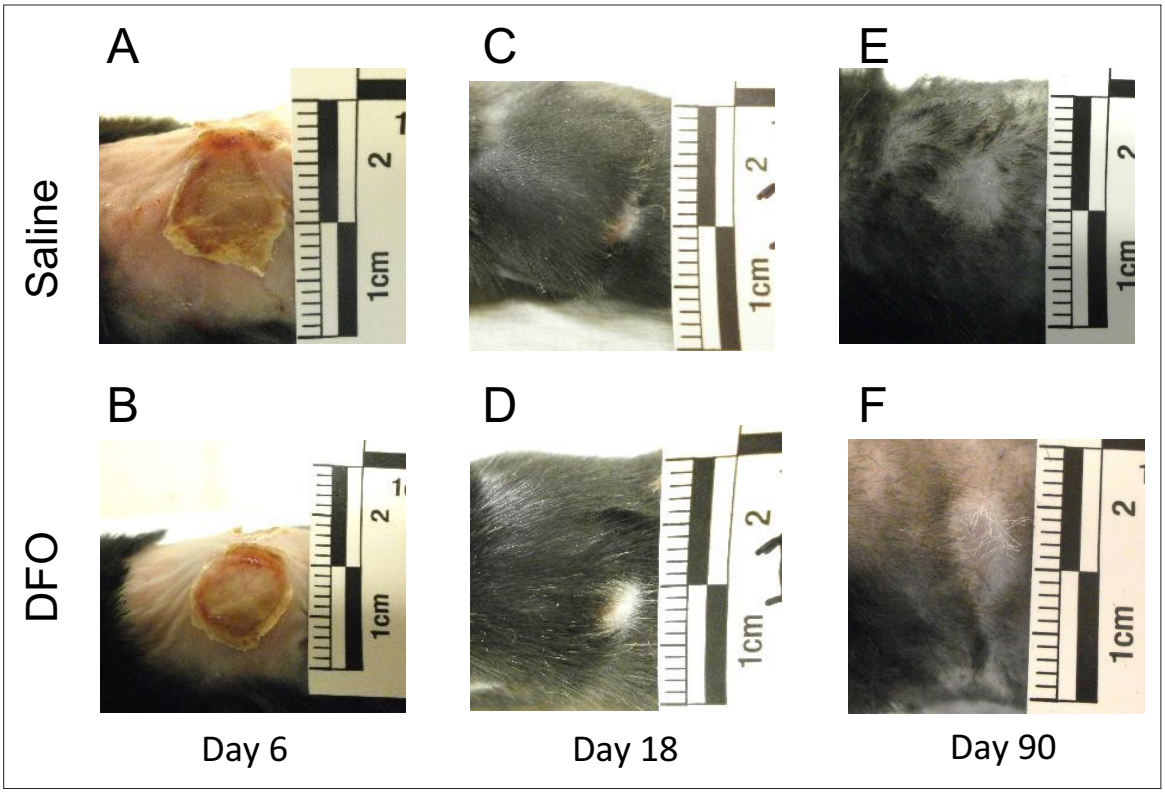

Figure 5—figure supplement 2. Deferoxamine (DFO) treatment did not significantly affect external wound sizes nor times to wound closure. (**A–F**) Photographs of the external wounds of saline- versus DFO-treated mice at (**A, B**) 6, (**C, D**) 18, and (**E–, F**) 90 d after injury.

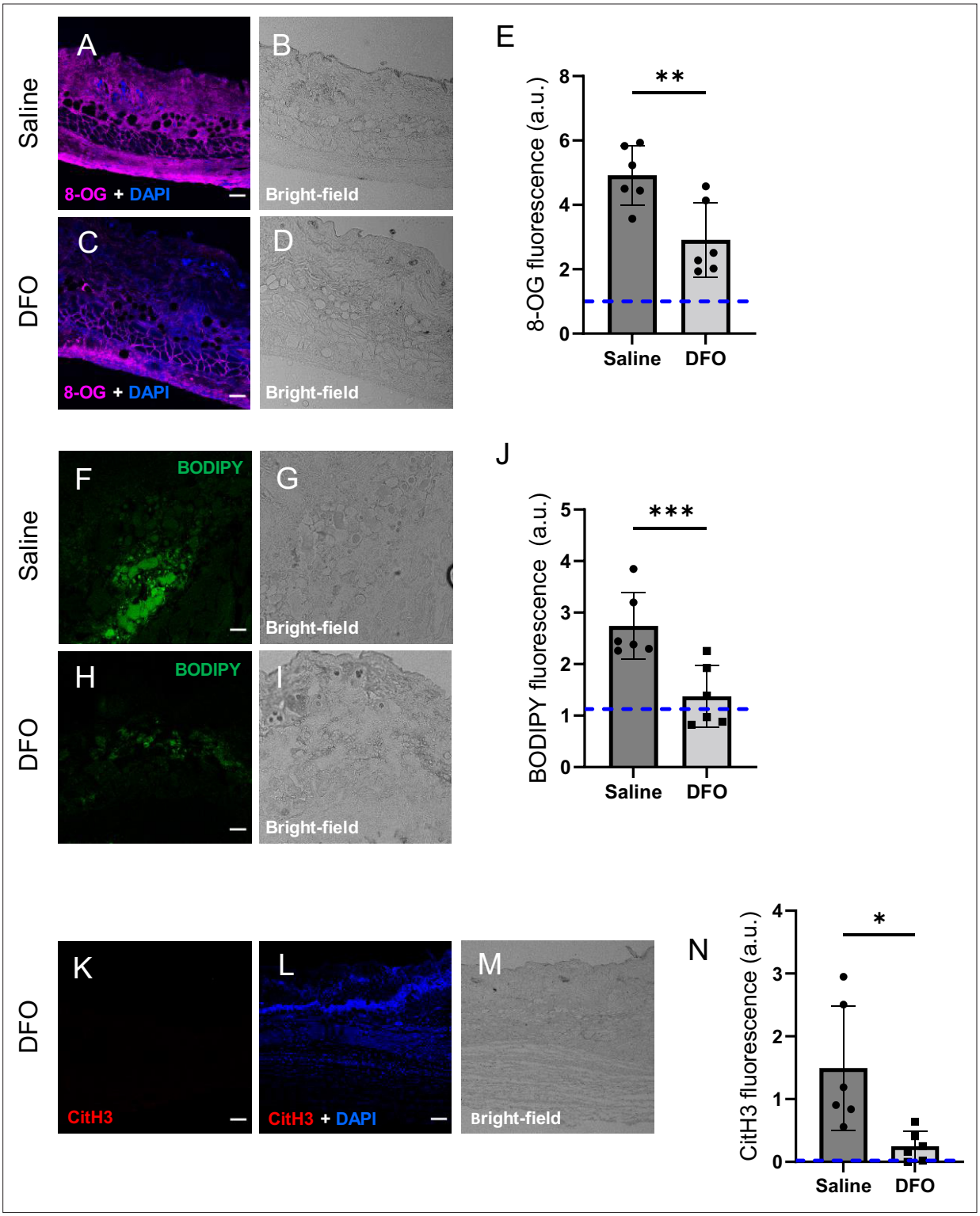

Figure 6. Deferoxamine (DFO) treatment improved the muscle pressure injury (mPI) microenvironment at early time point (day 3). (**A–D**) Immunostaining of 8-OG (for DNA damage) in saline-treated versus DFO-treated mPI. Nuclei were stained blue with DAPI. (**B**) and (**D**) are brightfield images of (**A**) and (**C**), respectively. (**E**) Quantification of 8-OG. (**F–I**) BODIPY staining (for lipid peroxidation) and brightfield in saline- versus DFO-treated mPI. (**J**) Quantification of BODIPY. (**K**) CitH3 immunostaining (**L**) with DNA/nuclear co-stain and (**M**) brightfield in DFO-treated mPI at day 3. (**N**) Quantification of CitH3 staining in DFO-treated versus the saline-treated mPI, which was analyzed in ***Figure 2F and G***. Scale bars: 50 µm. Blue dashed lines refer to mean fluorescence intensities for uninjured dorsal skinfolds. All quantitative data are reported as means ± SD. n = 6 mice. *<0.05, **<0.01, ***<0.001. Statistical significance in (**E**), (**J**), and (**N**) was computed by paired Student's *t* test.

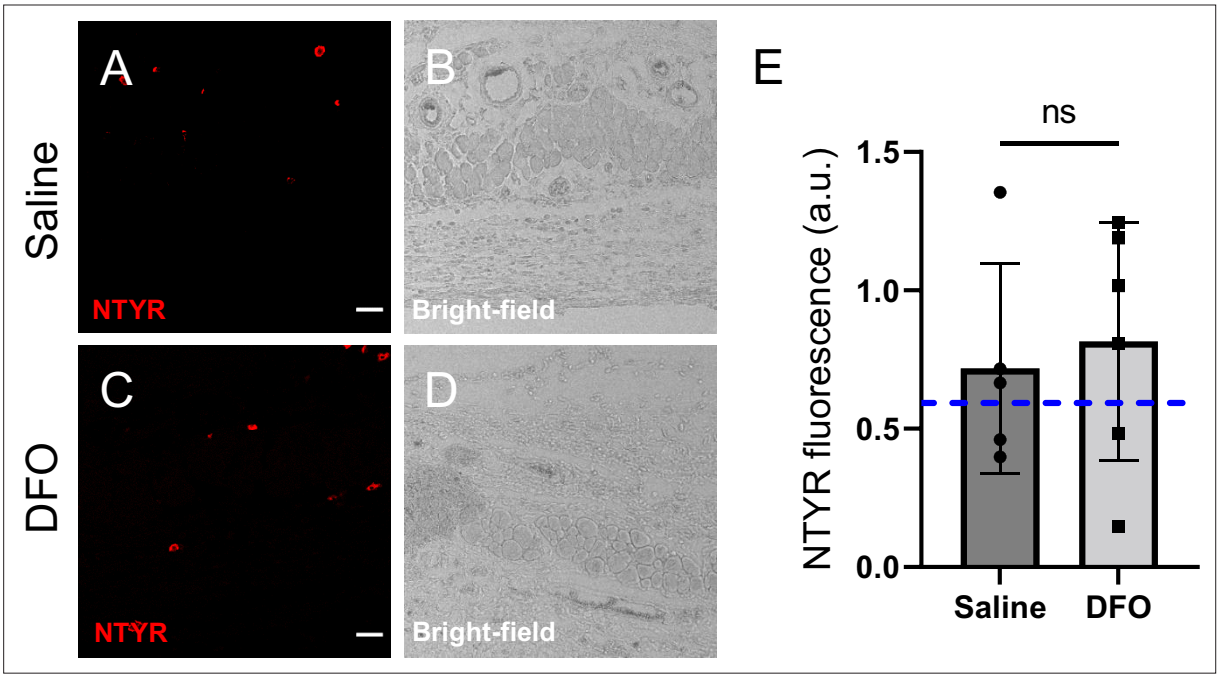

Figure 6—figure supplement 1. Nitroxidative stress in deferoxamine (DFO) versus saline-treated tissues 3 d after muscle pressure injury (mPI). (**A–D**) Immunostaining of nitrotyrosine (NTYR), a marker of protein nitration and nitroxidative stress, in saline- versus DFO-treated wound tissues. (**B**) and (**D**) are brightfield images of (**A**) and (**C**), respectively. Scale bars are 50 μm. (**E**) Quantification of NTYR staining. Blue dotted line indicates average NTYR fluorescence in uninjured skinfold. Mean ± SD. n = 6 mice. ns, not significant. Statistical significance was computed by unpaired Student's *t* test.

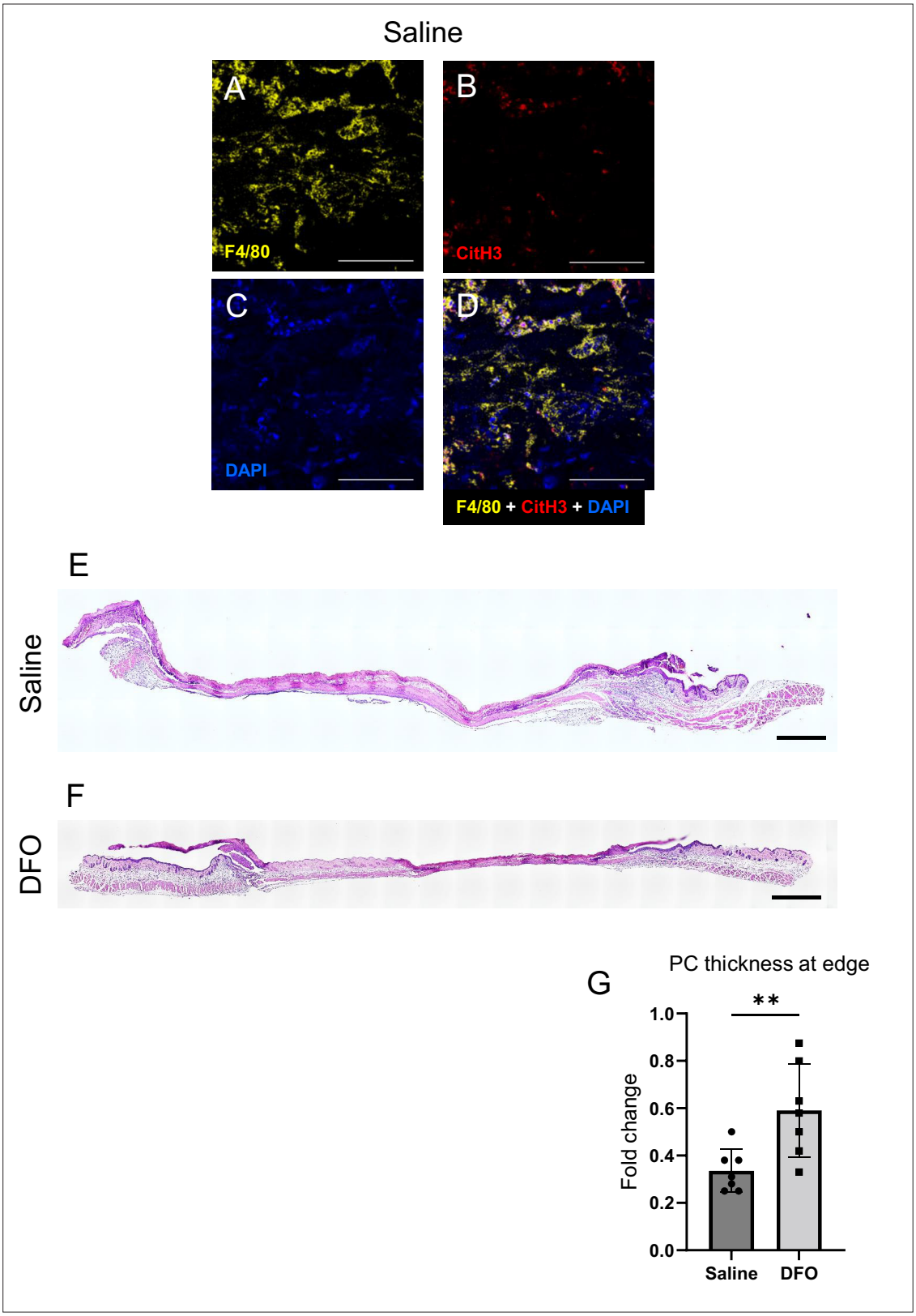

Figure 6—figure supplement 2. Injury response at day 3 after pressure. (**A**) Immunostaining in yellow for F4/80 receptor (a pan-macrophage marker), (**B**) CitH3, a marker of extracellular traps, in red and (**C**) DAPI nuclear stain. (**D**) Merge of (**A**), (**B**), and (**C**). All images were collected from saline-treated muscle pressure injury (mPI) at day 3 post-injury. Laser excitations were sequential, not simultaneous, using 555 nm for yellow, and 594 nm for red. Scale bars are 50 μm. H&E-stained wound sections of (**E**) saline- and (**F**) deferoxamine (DFO)-treated mPI at 3 d. Scale bars are 1000 μm. (**G**) Another

Figure 6—figure supplement 2 continued on next page

Figure 6—figure supplement 2 continued

difference between DFO and saline at day 3 was the thickness of the panniculus carnosus (PC) at the edge of the wound. This might reflect edema. Mean ± SD. n = 7 mice. **<0.01. Statistical significance was computed by paired Student's *t* test.

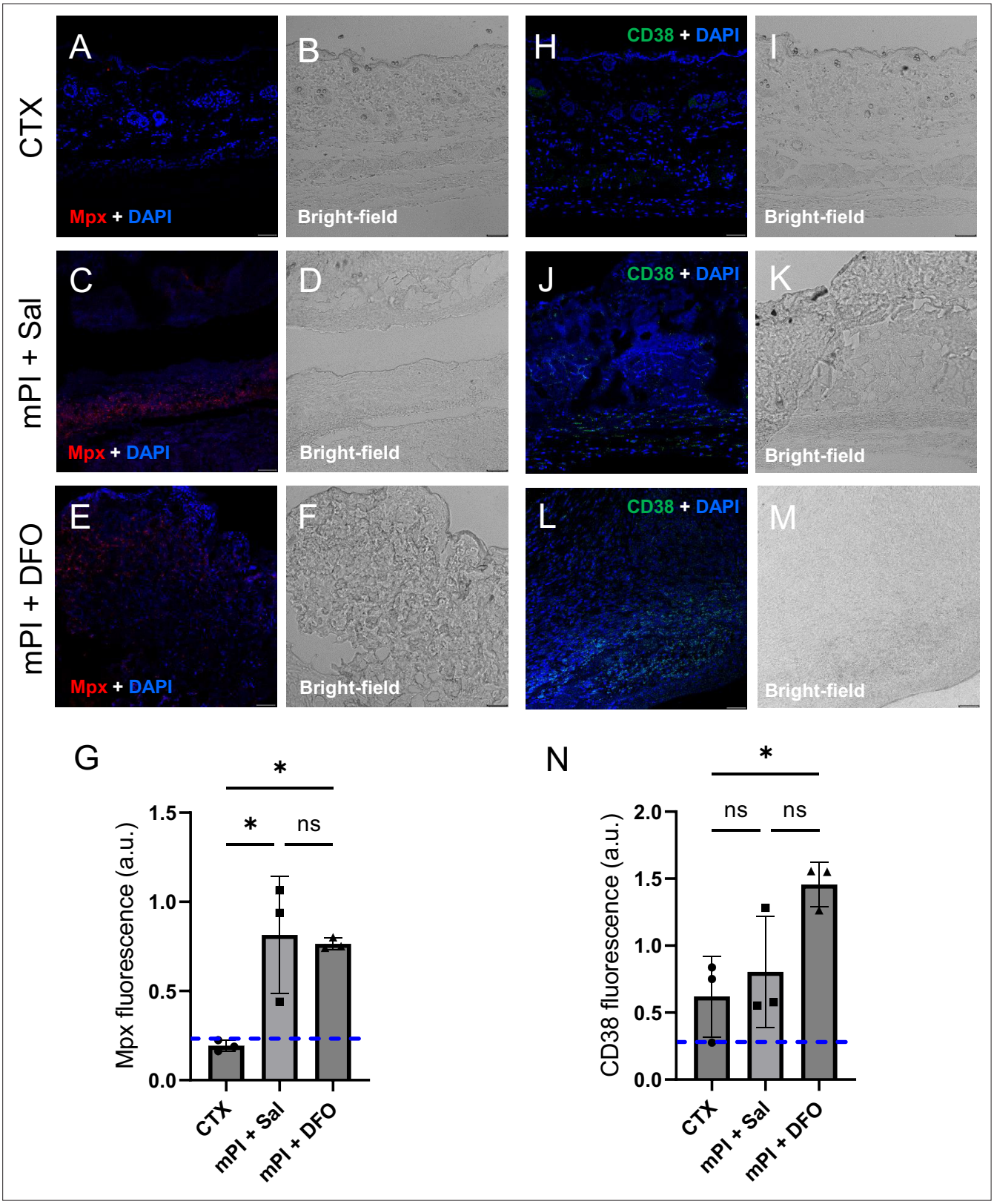

Figure 6—figure supplement 3. Comparing immune markers in cardiotoxin (CTX)-injured tissue, saline-treated muscle pressure injury (mPI), and deferoxamine (DFO)-treated mPI. (**A–F**) Immunostaining of myeloperoxidase (Mpx), a marker of neutrophil extracellular traps (NETs/NETosis), in CTX, saline-treated mPI and DFO-treated mPI tissues. (**B**), (**D**), and (**F**) are brightfield images of (**A**), (**C**), and (**E**), respectively. (**G**) Quantification of Mpx staining. (**H–M**) Immunostaining of CD38, a marker of CD4+, CD8+, B, and natural killer cells, in CTX, saline-treated mPI and DFO-treated mPI tissues.

Figure 6—figure supplement 3 continued on next page

Figure 6—figure supplement 3 continued

(**I**), (**K**), and (**M**) are brightfield images of (**H**), (**J**), and (**L**), respectively. Scale bars are 50 μm. (**N**) Quantification of CD38 staining. Mean ± SD. n = 3 mice. *<0.05. Statistical significance was computed by one-way analysis of variance (ANOVA) with Tukey's post hoc test.

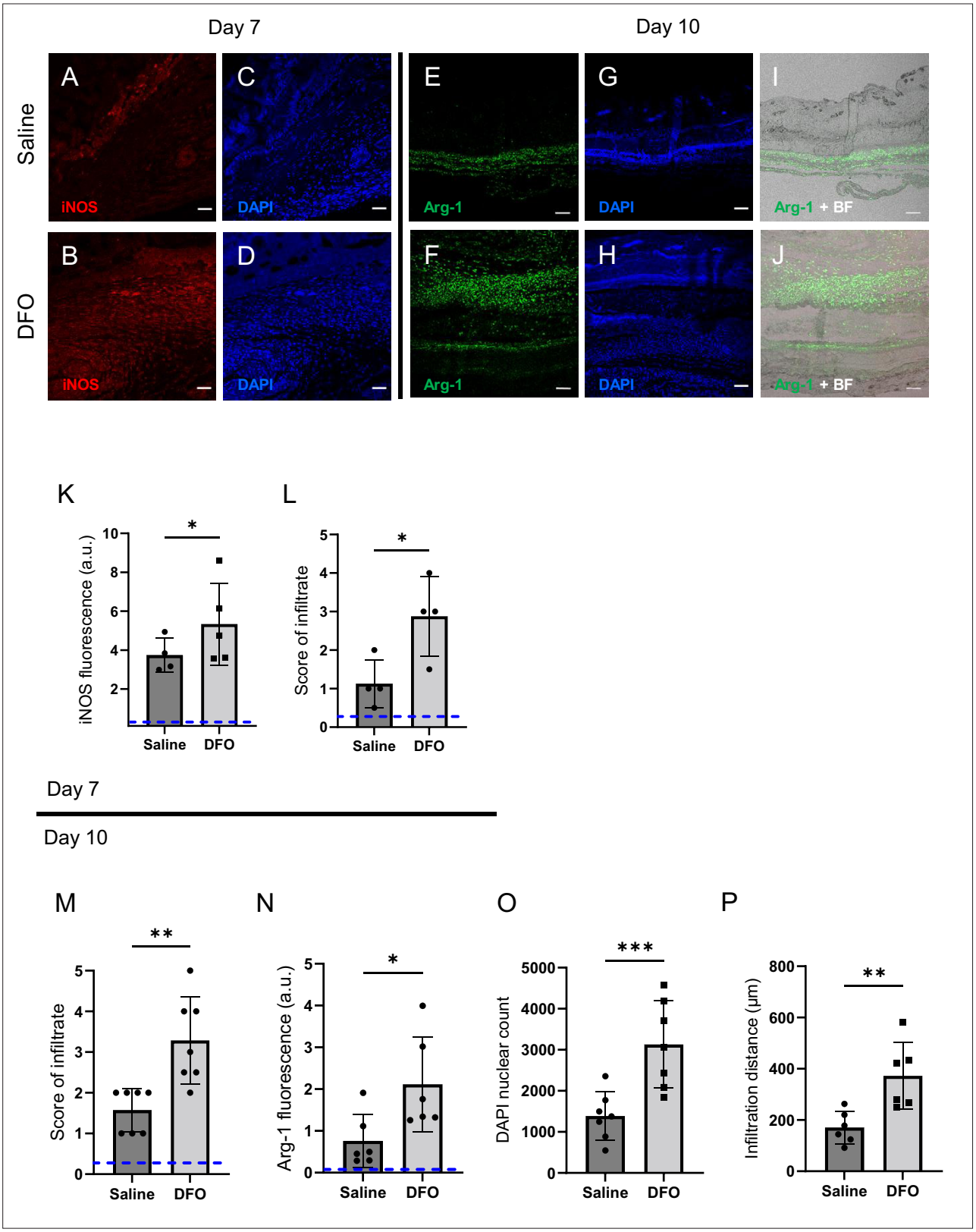

Figure 7. Deferoxamine (DFO) treatment improved immune infiltration (7 and 10 d after muscle pressure injury [mPI]). (**A, B**) Immunostaining of inducible nitric oxide synthase (iNOS, associated with pro-inflammatory activation) in saline- versus DFO-treated mPI at day 7 post-injury. (**C, D**) Nuclei are stained blue with DAPI to show the count of infiltrating cells. (**E, F**) Immunostaining of Arginase-1 (Arg-1) in saline- versus DFO-treated mPI at day 10 post-injury. (**G, H**) Nuclei are co-stained blue with DAPI. (**I, J**) Merged brightfield and Arg-1 immunostaining. (**K**) Quantification of iNOS staining at day 7

Figure 7 continued on next page

Figure 7 continued

between saline- and DFO-treated. (**L**) Scoring of immune infiltrate into the injured tissue at day 7. (**M**) Scoring of immune infiltrate into the injured tissue at day 10. (**N**) Quantification of Arg-1 staining. (**O**) Count of DAPI nuclei. (**P**) Distance of tissue infiltrated by Arg-1+ cells in saline- versus DFO-treated tissues. Scale bars: 50 μm. Blue dashed lines refer to histology scores and mean fluorescence intensities for uninjured dorsal skinfolds. All quantitative data are reported as means ± SD. n = 4–7 mice. *<0.05, **<0.01, ***<0.001. Statistical significance in (**K–P**) was computed by paired Student's *t* test.

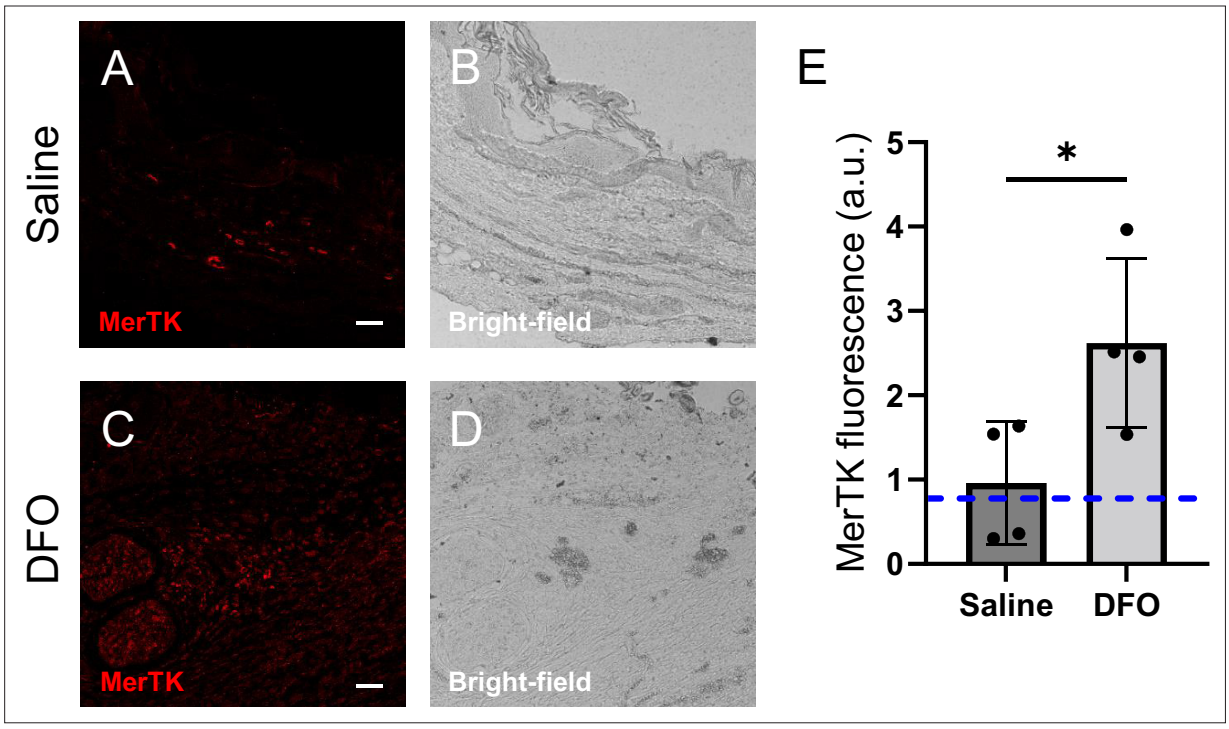

Figure 7—figure supplement 1. Immune infiltration and function in deferoxamine (DFO) versus saline-treated tissues 7 d after muscle pressure injury (mPI). (**A–D**) Immunostaining of MerTK, a marker of macrophage phagocytosis, in saline- versus DFO-treated wound tissues. (**B**) and (**D**) are brightfield images of (**A**) and (**C**), respectively. Scale bars are 50 μm. (**E**) Quantification of MerTK staining. Mean ± SD. n = 4 mice. *<0.05. Statistical significance was computed by paired Student's *t* test.

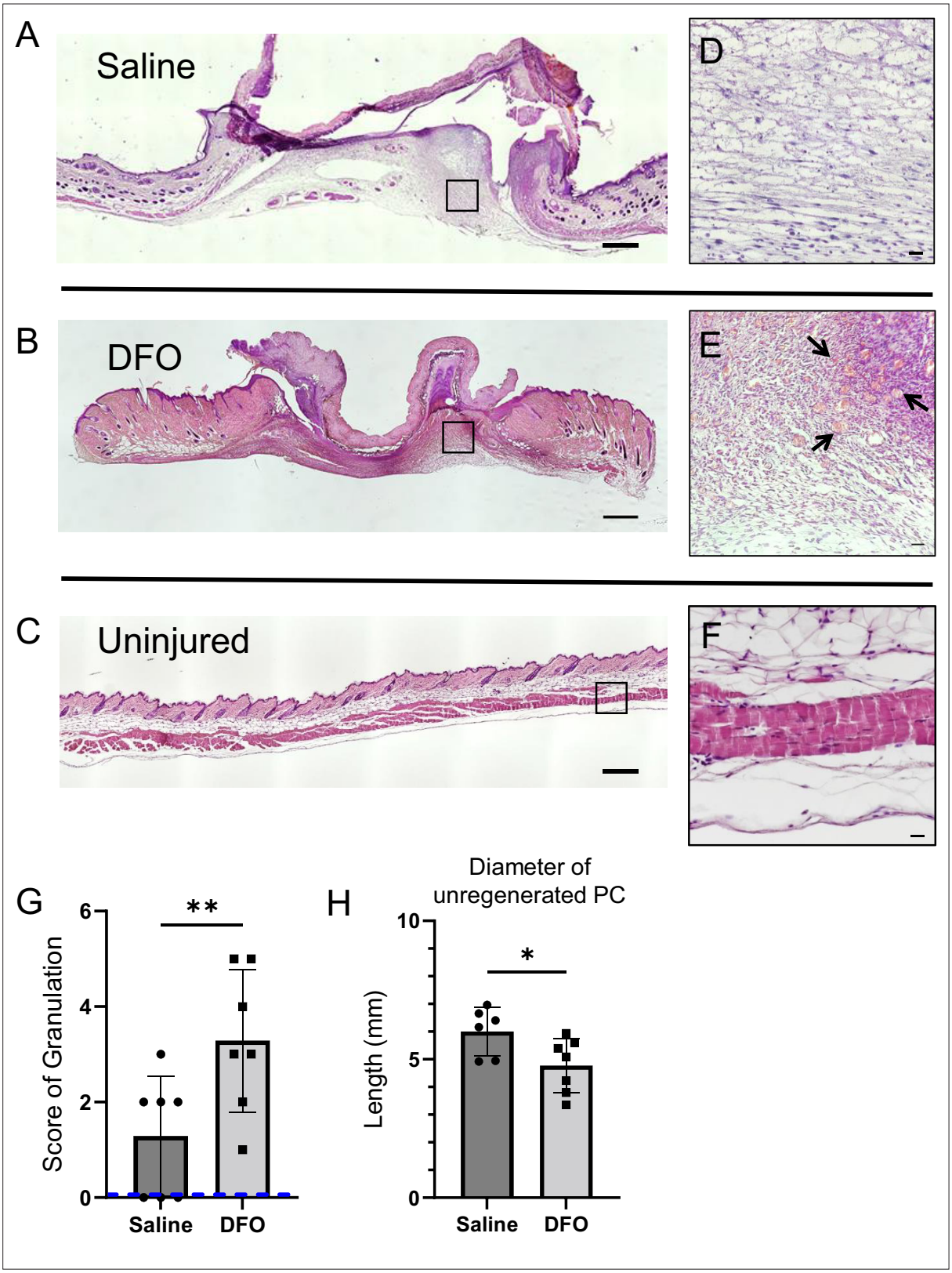

Figure 7—figure supplement 2. Deferoxamine (DFO) treatment improved angiogenesis and granulation following muscle pressure injury (mPI). Cross-sections of (**A**) saline-treated and (**B**) DFO-treated mPI with surrounding margins, at 10 d post-injury, stained with H&E. (**C**) Cross-section of healthy uninjured skinfold, stained with H&E. Scale bars are 500 µm. (**D–F**) Close-ups of (**A–C**), respectively. Arrows point to new capillaries of granulation tissue. Scale bars are 10 µm. (**G**) Histopathology scoring of granulation in saline- versus DFO-treated mPI at day 10. (**H**) Diameter of the unregenerated

Figure 7—figure supplement 2 continued on next page

Figure 7—figure supplement 2 continued

panniculus carnosus (PC) (diameter of hole) of DFO-treated tissues versus saline 10 d after mPI. Mean ± SD. n = 6–7 mice. *<0.05, **<0.01. Statistical significance was computed by paired Student's *t* test.

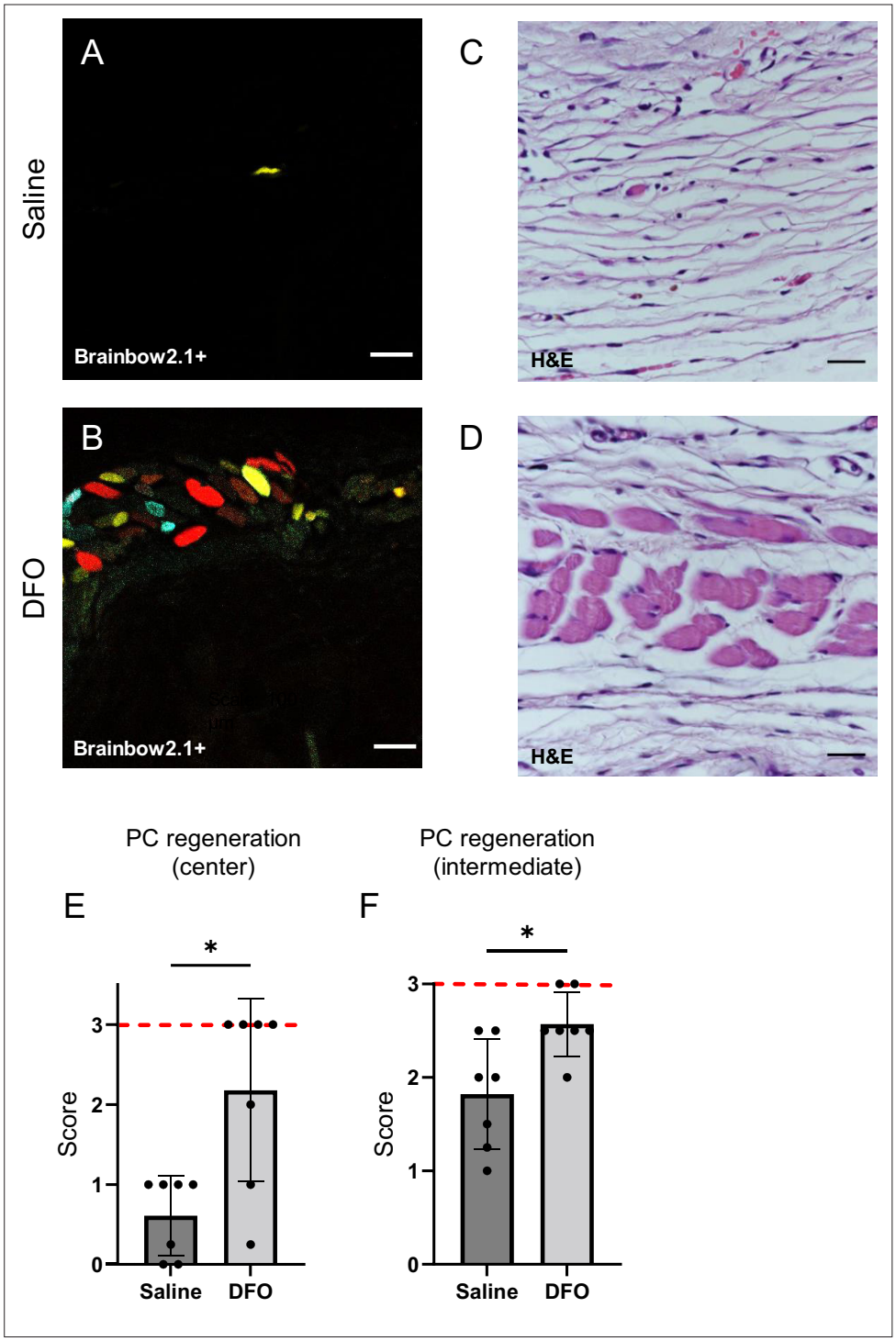

Figure 8. Deferoxamine (DFO) increased the extent of muscle regeneration at day 40. (**A, B**) Confocal fluorescent and (**C, D**) H&E-stained cross-sections of regenerated muscle fibers from saline- and DFO-treated muscle pressure injury (mPI), 40 d post-injury. Scale bars: 100 μm. (**E, F**) Histological scoring of panniculus carnosus (PC) muscle regeneration in saline- and DFO-treated mPI versus acute cardiotoxin (CTX)-injured tissues at the center and edge of the wound, 40 d post-injury. Red dashed lines refer to PC regeneration scores at center and intermediate regions after CTX injury at day 40. All quantitative data are reported as means ± SD. n = 7 mice. *<0.05, **<0.01. Statistical significance in (**E, F**) was computed by paired Student's *t* test.

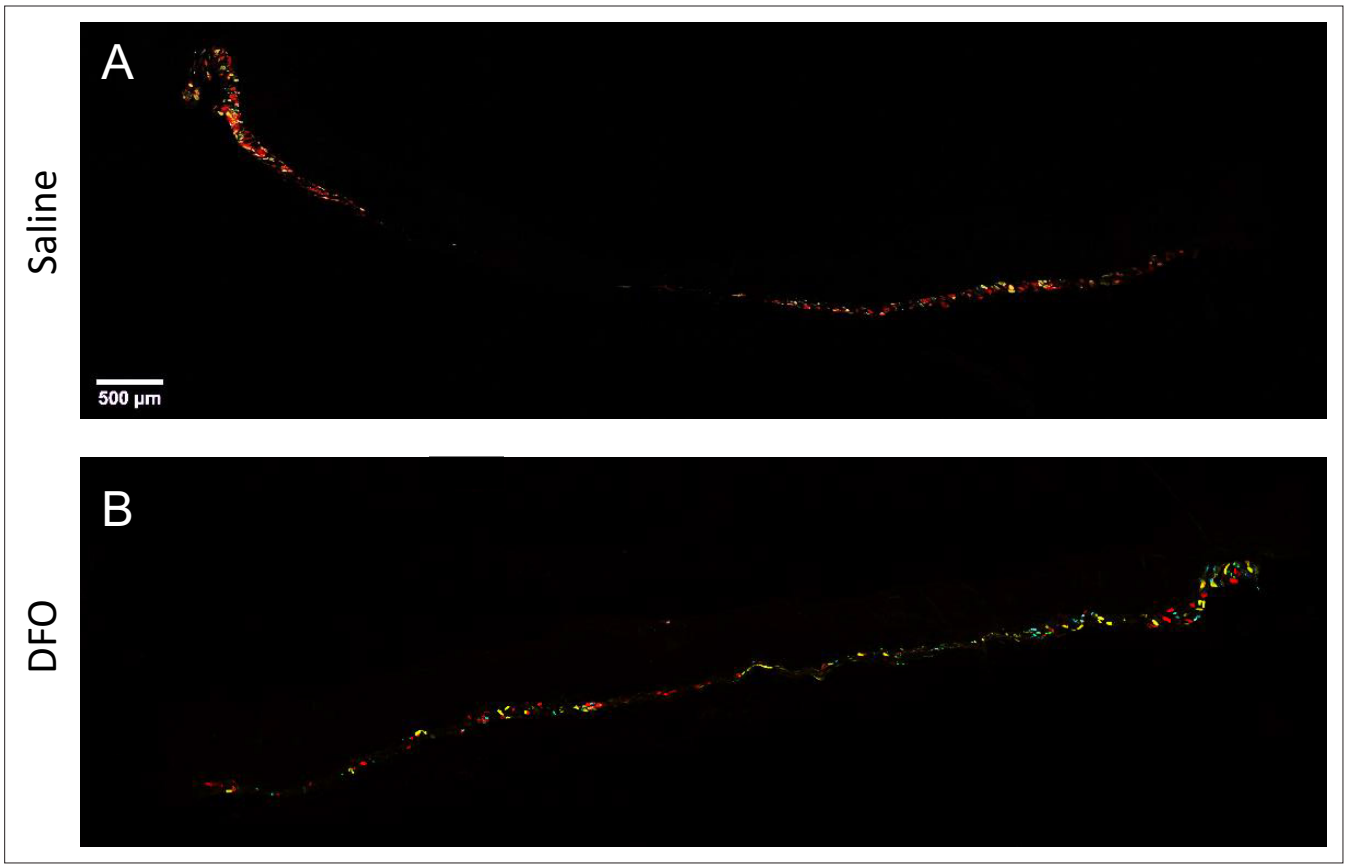

Figure 8—figure supplement 1. Failure of muscle regeneration after muscle pressure injury (mPI) is ameliorated by deferoxamine (DFO) treatment. (**A, B**) Confocal fluorescent imaging of wound cross-sections from (**A**) saline- and (**B**) DFO-treated samples, 40 d post-injury, showing the presence or absence of regenerated myofibers via confetti fluorescence in the *panniculus carnosus* muscle.

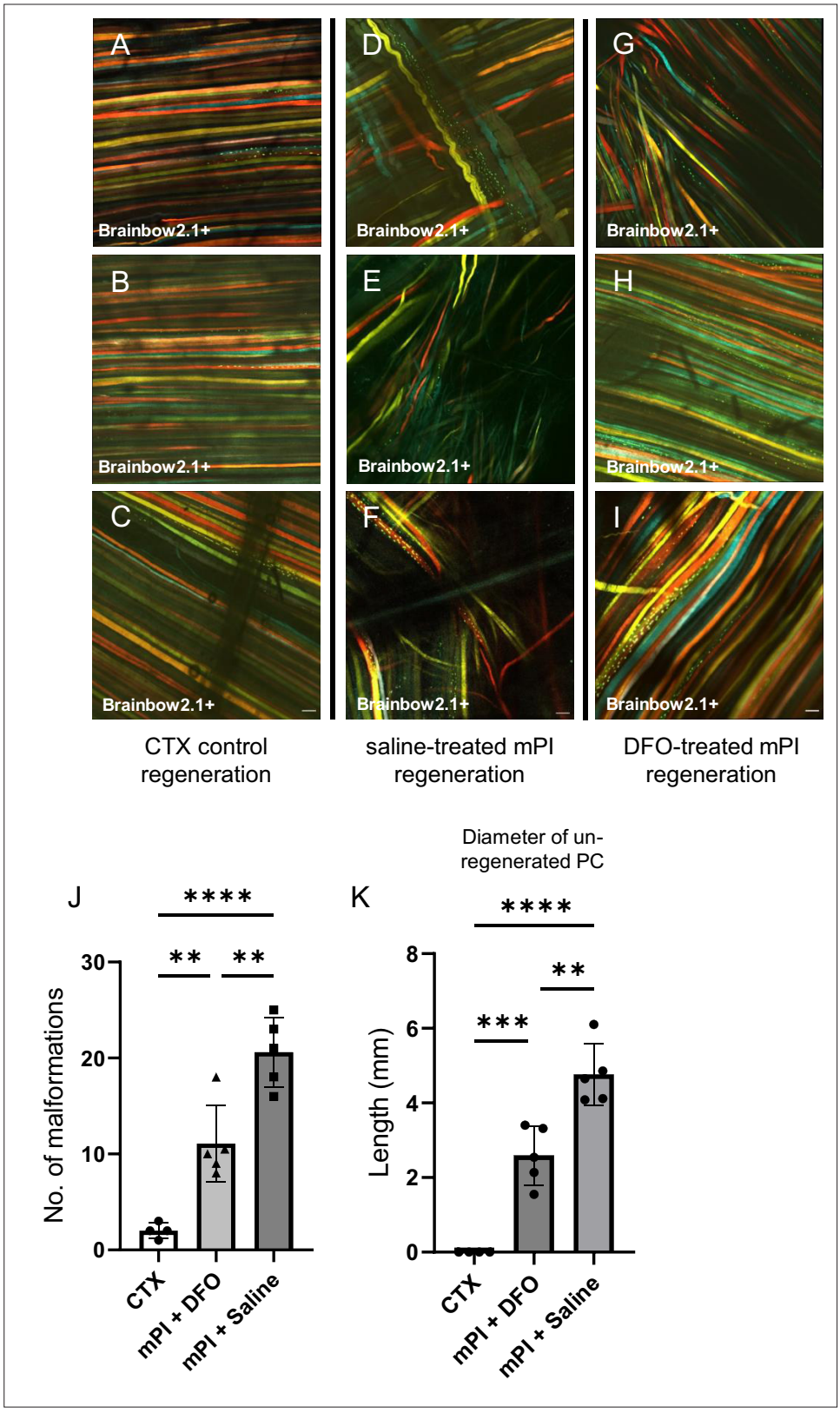

Figure 9. Deferoxamine (DFO) improved muscle morphology. Confocal microscopy of confetti-labeled muscle regeneration in ex vivo tissue blocks. Note that unlabeled tissue types such as blood vessels and hair create black shadows on top of the images. (**A–C**) Left column shows healthy regeneration in the control condition, toxin-induced injury, at 40 d. Experiment was halted at 40 d for cardiotoxin (CTX) only due to complete regeneration.

Figure 9 continued on next page

Figure 9 continued

(**D–F**) Middle column shows regenerated muscle fibers of saline-treated muscle pressure injury (mPI), 90 d post-injury. Note the presence of non-parallel fibers, bent fibers, and split fibers (i.e., fibers with one or more branches). (**G–I**) Right column shows regenerated muscle fibers of DFO-treated mPI, 90 d post-injury. Scale bars: 100 μm. (**J**) Quantification of muscle fiber malformations. (**K**) Diameter of gap (unregenerated region) in panniculus carnosus (PC) muscle layer at day 90 post-mPI between saline- and DFO-treated wounds. All quantitative data are reported as means ± SD. n = 4–5 mice. **<0.01, ***<0.001, ****<0.0001. Statistical significance in (**J, K**) was computed by one-way ANOVA with Tukey's post hoc test.